European Commission

J R C T E C H N I C A L R E P O R T S

Calculation of Blast Loads for Application to Structural Components

Administrative Arrangement N° JRC 32253-2011 with DG-HOME
Activity A5 - Blast Simulation Technology Development

Vasilis KARLOS
George SOLOMOS

2013

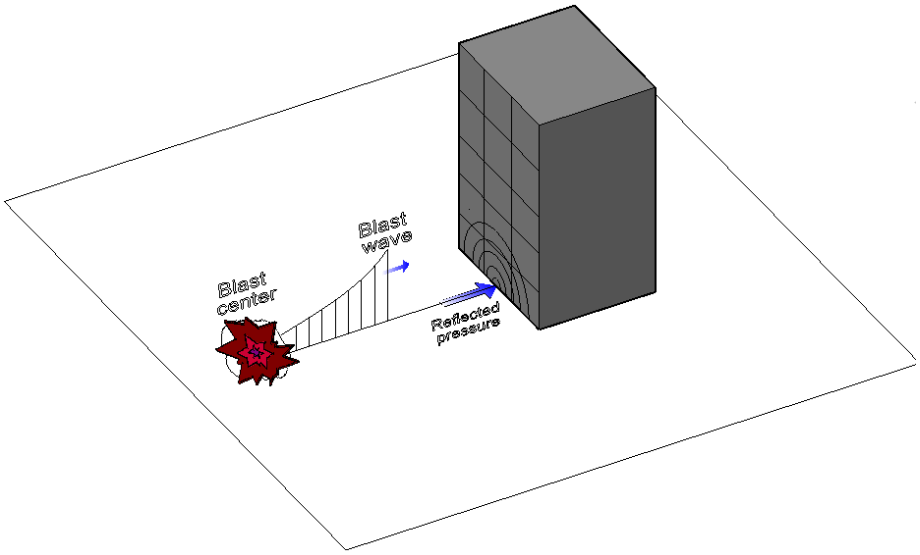

Report EUR 26456 EN

Joint Research Centre

European Commission
Joint Research Centre
Institute for the Protection and Security of the Citizen

Contact information
George Solomos
Address: Joint Research Centre, Via Enrico Fermi 2749, TP 480, 21027 Ispra (VA), Italy
E-mail: george.solomos@jrc.ec.europa.eu
Tel.: +39 0332 78 9916
Fax: +39 0332 78 9049

http://ipsc.jrc.ec.europa.eu/
http://www.jrc.ec.europa.eu/

Legal Notice
Neither the European Commission nor any person acting on behalf of the Commission is responsible for the use which might be made of this publication.

Europe Direct is a service to help you find answers to your questions about the European Union
Freephone number (*): 00 800 6 7 8 9 10 11
(*) Certain mobile telephone operators do not allow access to 00 800 numbers or these calls may be billed.

A great deal of additional information on the European Union is available on the Internet.
It can be accessed through the Europa server http://europa.eu/.

JRC 87200

EUR 26456 EN

ISBN 978-92-79-35158-7

ISSN 1831-9424

doi:10.2788/61866

Luxembourg: Publications Office of the European Union, 2013

© European Union, 2013

Reproduction is authorised provided the source is acknowledged.

Printed in Italy

Calculation of Blast Loads for Application to Structural Components

Administrative Arrangement N^{o} JRC 32253-2011 with DG-HOME

Activity A5 - Blast Simulation Technology Development

Vasilis KARLOS

George SOLOMOS

European Laboratory for Structural Assessment

December 2013

Contents

1. **Introduction** 1

2. **Explosions and blast waves** 2

2.1 Ideal blast wave characteristics 2
2.2 Scaling laws 4
2.3 Explosive type and weight 5
2.4 Explosion and blast-loading types 7
2.5 Blast wave reflection 8
2.6 Surface burst and loading 15
2.7 Effect of finite reflecting surface 16
2.8 Dynamic pressure 17

3. **Calculation of structural blast loads** 18

3.1 Blast pressure determination 18
3.2 Calculation of pressure loads on building surfaces 24
3.3 Influence of openings 32
3.4 Combination rules 33

4. **Summary of the blast loads calculation** 34

5. **Case studies** 37

5.1 Blast parameter calculation examples 37
5.2 Blast wave pressure loads for a small structure 40
5.3 Blast wave pressure loads for element design 46

6. **Conclusions** 49

7. **References** 49

1. Introduction

Over the last decades considerable attention has been raised on the behaviour of engineering structures under blast or impact loading. The use of explosives by terrorist groups around the world that target civilian buildings and other structures is becoming a growing problem in modern societies. Explosive devices have become smaller in size and more powerful than some years ago, leading to increased mobility of the explosive material and larger range effects. Usually the casualties from such a detonation are not only related to instant fatalities as a consequence of the direct release of energy, but mainly to structural failures that might occur and could result in extensive life loss. Famous examples of such cases are the bombing attacks at the World Trade Center in 1993 and on the Alfred P. Murrah Federal Building in Oklahoma City in 1995. In both of these incidents, structural failure, including glass breakage, resulted in far more victims and injuries than the blast wave itself. After the events of the 11th September 2001 that led to the collapse of the World Trade Center in New York it was realized that civilian and government buildings, as well as areas with high people concentration (metro and train stations, means of mass transportation, stadiums etc.) are becoming potential bombing targets of terrorist groups. Since most engineering structures are vulnerable to such type of loading scenarios, a guide should be introduced to the designer in order to guarantee structural integrity even under those extreme situations.

The problem of structural resistance under explosive loads has been under investigation for many years and has been well advanced in the military community. This is also the reason that the majority of these findings are not accessible to the public and are only restricted to military use. Nevertheless, some documentation that allows the prediction of the effects of an explosive blast is available for use by design engineers. The Eurocode EN 1991-1-7 [1] makes reference to the case of accidental loads and explosions, but it is mainly focused on impact actions, such as collisions from trucks, trains, ships, helicopters or any other vehicle in general. Reference is also made to gas explosions that take place in enclosed spaces but an overall approach for design under blast external loads is still missing. Some design strategies are also recommended aiming to ensure increased robustness in building structures that are to endure localized failure. However, no guidelines are provided in EN 1991-1-7 for the calculation of external blast induced loads.

Of the several informative sources that can be found in the open literature [2-6] the most reliable and quoted references to date appear to be some USA military publications, and in particular a Technical Report [7] by Kingery and Bulmash (1984) and the Army Technical Manual 5-1300 [8]. This latter provides detailed information and procedures for the design of structures to resist the effects of explosions, it is periodically updated and a more functional version of it is currently (Dec.2008) available [9].

The development of a procedure that will give practical design solutions is essential for the design of new or the retrofitting of existing structures so as to be able to withstand the effects of explosive loads. The engineer needs to calculate the acting forces according to a certain blast scenario, which includes the type and weight of the used explosive, the

distance from the structure and the geometry of the surrounding area and the structure itself. These forces should then be applied on the structural system at hand in order to design structural members, sections and connections that will ensure sufficient robustness of the building to survive the effects of the computed actions.

In the current technical guide, an overview of a design procedure for structures under blast loading is provided. The material presented has been collected from various sources and mainly from references [7-9]. The analysis focuses on ways to estimate blast loading on structures and, to a lesser extent, on their response under such types of actions. Indicative examples of structures under explosive loads are also analyzed in order to provide designers practical guidance on how to deal with similar cases.

2. Explosions and blast waves

2.1 Ideal blast wave characteristics

An explosion can be defined as a very fast chemical reaction involving a solid, dust or gas, during which a rapid release of hot gases and energy takes place. The phenomenon lasts only some milliseconds and it results in the production of very high temperatures and pressures. During detonation the hot gases that are produced expand in order to occupy the available space, leading to wave type propagation through space that is transmitted spherically through an unbounded surrounding medium. Along with the produced gases, the air around the blast (for air blasts) also expands and its molecules pile-up, resulting in what is known as a blast wave and shock front. The blast wave contains a large part of the energy that was released during detonation and moves faster than the speed of sound.

Figure 1 shows the idealised profile of the pressure in relation to time for the case of a free-air blast wave, which reaches a point at a certain distance from the detonation. The pressure surrounding the element is initially equal to the ambient pressure P_o, and it undergoes an instantaneous increase to a peak pressure P_{so} at the arrival time $t_{A,}$ when the shock front reaches that point. The time needed for the pressure to reach its peak value is very small and for design purposes it is assumed to be equal to zero. The peak pressure P_{so} is also known as **side-on overpressure** or **peak overpressure**. The value of the peak overpressure as well as the velocity of propagation of the shock wave decrease with increasing distance from the detonation center. After its peak value, the pressure decreases with an exponential rate until it reaches the ambient pressure at t_A+t_o, t_o being called the positive phase duration. After the positive phase of the pressure-time diagram, the pressure becomes smaller (referred to as negative) than the ambient value, and finally returns to it. The negative phase is longer than the positive one, its minimum pressure value is denoted as P_{so}^- and its duration as t_o^-. During this phase the structures are subjected to suction forces, which is the reason why sometimes during blast loading glass fragments from failures of facades are found outside a building instead in its interior.

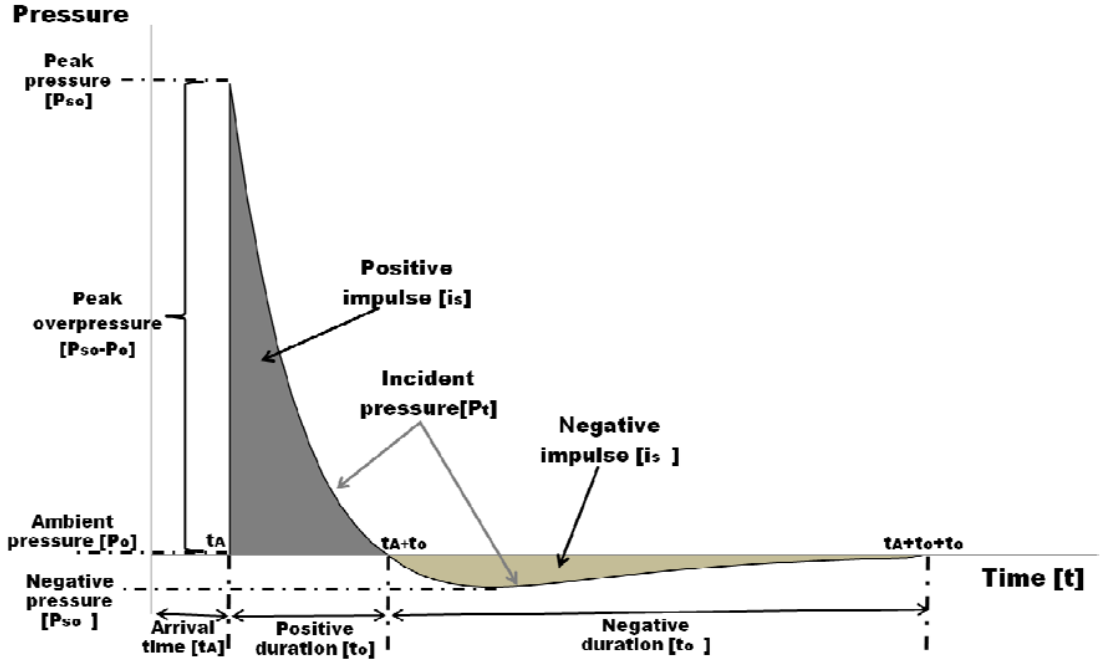

Figure 1: Ideal blast wave's pressure time history

The negative phase of the explosive wave is usually not taken into account for design purposes as it has been verified that the main structural damage is connected to the positive phase. Additionally, the pressures that are produced from the negative phase of the blast wave are relatively small compared to those of the positive phase and since these are in the opposite direction, it is usually on the safe side to assume that they do not have a big impact on the structural integrity of buildings under blast loads. However, the pressures that are below the ambient pressure value should be taken into account if the overall structural performance of a building during a blast is assessed and not only its structural integrity.
As can be seen from Figure 1, the positive incident pressure decreases exponentially. The following form of Friedlander's equation has been proposed [2], and is widely used to describe this rate of decrease in pressure values:

$$P_s(t) = P_{so}\left(1 - \frac{t}{t_o}\right)e^{-b\frac{t}{t_o}} \tag{1}$$

where, P_{so} is the peak overpressure,
t_o is the positive phase duration,
b is a decay coefficient of the waveform and
t is the time elapsed, measured from the instant of blast arrival.

The decay coefficient b can be calculated through a non-linear fitting of an experimental pressure time curve over its positive phase. Besides the peak pressure, for design purposes an even more important parameter of the blast wave pulse is its **impulse** because it relates to the total force (per unit area) that is applied on a structure due to the blast. It is defined as the shaded area under the overpressure-time curve of Figure 1. The impulse is distinguished into positive i_s and negative i_s^-, according to the relevant phase of the blast wave time history. Equation (2) gives the expression in the case of the positive impulse,

which is more significant than its negative counterpart in terms of building collapse prevention,

$$i_s = \int_{t_A}^{t_A+t_o} P_s(t)\,dt \tag{2}$$

For the above Friedlander equation (1), the positive impulse can be analytically calculated as

$$i_s = \frac{P_{so} t_o}{b^2}\left[b - 1 + e^{-b})\right] \tag{3}$$

This equation constitutes an alternative way for solving iteratively for the decay parameter *b* when the values of the i_s, P_{so} and t_o are known from experimental data.

2.2 Scaling laws

One of the most critical parameters for blast loading computations is the distance of the detonation point from the structure of interest. The peak pressure value and velocity of the blast wave, which were described earlier, decrease rapidly by increasing the distance between the blast source and the target surface, as shown in Figure 2. In the figure only the positive phases of the blast waves are depicted, whose durations are longer whenever the distance from the detonation point increases.

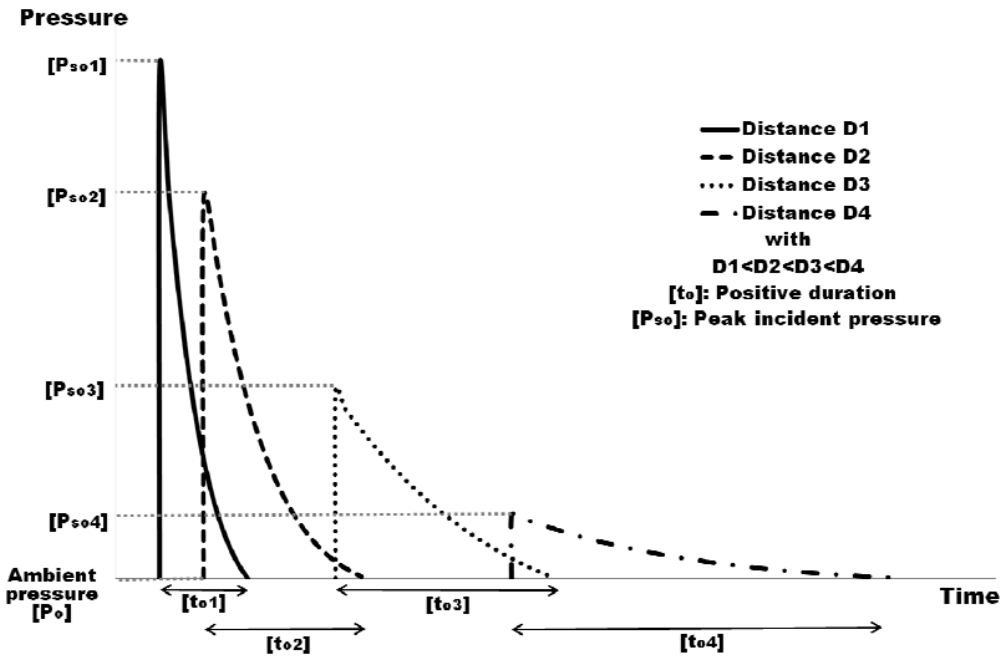

Figure 2: Influence of distance on the blast positive pressure phase.

The effect of distance on the blast characteristics can be taken into account by the introduction of scaling laws. These laws have the ability to scale parameters, which were

defined through experiments, in order to be used for varying values of distance and charge energy release. The experimental results are, in this way, generalized to include cases that are different from the initial experimental setup. The most common blast scaling laws are the ones introduced by Hopkinson-Cranz and Sachs. The idea behind both formulations is that during the detonation of two charges of the same explosive that have similar geometry but different weight and are situated at the same scaled distance from a target surface, similar blast waves are produced at the point of interest as long as they are under the same atmospheric conditions. Sachs scaling is also suitable in the case of different atmospheric conditions. According to Hopkinson-Cranz law, a dimensional scaled distance is introduced as described by Equation (4),

$$Z = \frac{R}{\sqrt[3]{W}} \tag{4}$$

where, R is the distance from the detonation source to the point of interest [m] and
W is the weight (more precisely: the mass) of the explosive [kg].

Thus, suppose that an explosive charge of weight W_1 and characteristic size d_1, situated at distance R_1 from the point of interest, produces at this point a blast wave of peak overpressure P, impulse i_1, duration t_{o1}, with arrival time t_{a1} and that $R_1/\sqrt[3]{W_1} = \boldsymbol{\lambda}$. Then, what this scaling law implies is that a blast wave with the same peak overpressure P and similar form would be produced at this point by another explosive charge W_2 of characteristic dimension $d_2=\lambda d_1$, situated at distance $R_2=\lambda R_1$. Further, at the given point due to W_2 we would have: impulse $i_2=\lambda i_1$, duration $t_{o2}=\lambda t_{o1}$, and arrival time $t_{a2}=\lambda t_{a1}$.

It is essential to underline that under this formulation all distance and time parameters of a blast wave are scaled by the same factor $\boldsymbol{\lambda}$ but pressure and velocity values remain unchanged at similarly analogous times.

2.3 Explosive type and weight

In the present technical guide the focus will be on building structures, as these have proven to be the most common targets of terrorist attacks with the use of explosive devices. Nevertheless, the procedure that should be followed in the case of different structural elements is practically the same. The first step in designing a building to sustain blast loading is the definition of the type and weight of the explosive for which the design will be performed. Several types of explosives are available nowadays, any of which could be used for conducting an attack against a structure. In the majority of the cases solid explosives will be used in improvised explosive devices (IED), because of their transportability, relatively easy manufacturing and the possibility of their placement in vehicles that could be moved in the vicinity, adjacent or within (e.g. underground garages) a building.

The wide variety of explosives has led to the adoption of a universal quantity, which is used for all necessary computations of blast parameters. TNT (Trinitrotoluene) was chosen as its blast characteristics resemble those of most solid type explosives. An equivalent TNT weight is computed according to Equation (5) that links the weight of the chosen design

explosive to the equivalent weight of TNT by utilizing the ratio of the heat produced during detonation:

$$W_e = W_{exp} \frac{H^d_{exp}}{H^d_{TNT}} \tag{5}$$

where, W_e is the TNT equivalent weight [kg],

W_{exp} is the weight of the actual explosive [kg],

H^d_{exp} is the heat of detonation of the actual explosive [MJ/kg], and

H^d_{TNT} is the heat of detonation of the TNT [MJ/kg].

It is worth mentioning that approximately one third of the total chemical energy of the explosive is released by detonation. The rest is released at a slower rate as heat of combustion through burning of the explosive products mix with the surrounding air. Several tables that describe the heat output of most known explosives can be found in [8-9]. Table 1 provides estimates of the produced heat of detonation of some common explosives as defined in [8]. These values can be used for the calculation of the equivalent TNT weight with the use of Equation (5).

Table 1: Indicative values of heat of detonation of common explosives [6].

Name of explosive	Heat of detonation [MJ/kg]
TNT	4.10-4.55
C4	5.86
RDX	5.13-6.19
PETN	6.69
PENTOLITE 50/50	5.86
NITROGLYCERIN	6.30
NITROMETHANE	6.40
NITROCELLULOSE	10.60
AMON./NIT. (AN)	1.59

Table 2 shows some predetermined TNT equivalent weight factors as provided in [10]. These factors can be used to determine the weight of TNT that produces the same blast wave parameters as the ones from another explosive of certain weight. The comparison of these blast wave parameters can be done either for pressure or impulse values, so the following table contains two factors depending on the used method.

The weight of an explosive is usually estimated by taking into account a relevant attack scenario, which would involve a vehicle-borne or a personnel-borne improvised explosive device. Clearly, the larger the used vehicle that could be directed towards a structure, the larger the weight of the explosives it could carry leading to higher equivalent TNT weight values. In Table 3 an estimate of the quantity of explosives that could be transported by various vehicle types is presented. The engineer, following the relevant regulations and in consultation with the building owner, should decide on the type of explosive and size of vehicle that could be used for transportation, so as to be able to compute the equivalent

weight of TNT for which the structure should be designed. Due to a variety of such uncertainties, it is recommended to apply a safety factor to the charge weights and augment them by approximately 20%.

Table 2: Indicative TNT equivalent mass factors [10].

Name of explosive	TNT equivalent mass factor	
	Peak pressure	Impulse
TNT	1.00	1.00
C3	1.08	1.01
C4	1.37	1.19
CYCLOTOL	1.14	1.09
OCTOL 75/25	1.06	1.06
TETRYL	1.07	1.05
HMX	1.02	1.03
AMATOL	0.99	0.98
RDX	1.14	1.09
PETN	1.27	1.11

Table 3: Upper limit of charge weight per means of transportation.

Carrier	Explosive weight [kg]
Suitcase	10
Medium-sized car	200
Large-sized car	300
Pick-up truck	1400
Van	3000
Truck	5000
Truck with trailer	10000

2.4 *Explosion and blast-loading types*

Non-contact, unconfined explosions, external to a structure are considered in this report. As shown in Figure 3, they can be distinguished in three basic types, which depend on the relative position of the explosive source and the structure to be protected, i.e. on the height H^* above ground, where the detonation of a charge W occurs, and on the horizontal distance R_G between the projection of the explosive to the ground and the structure. These three explosion types are:

(a) ***Free-air bursts***: The explosive charge is detonated in the air, the blast waves propagate spherically outwards and impinge directly onto the structure without prior interaction with other obstacles or the ground.

(b) ***Air bursts***: The explosive charge is detonated in the air, the blast waves propagate spherically outwards and impinge onto the structure after having interacted first with the ground; a Mach wave front is created.

(c) ***Surface bursts***: The explosive charge is detonated almost at ground surface, the blast waves immediately interact locally with the ground and they next propagate hemi-spherically outwards and impinge onto the structure.

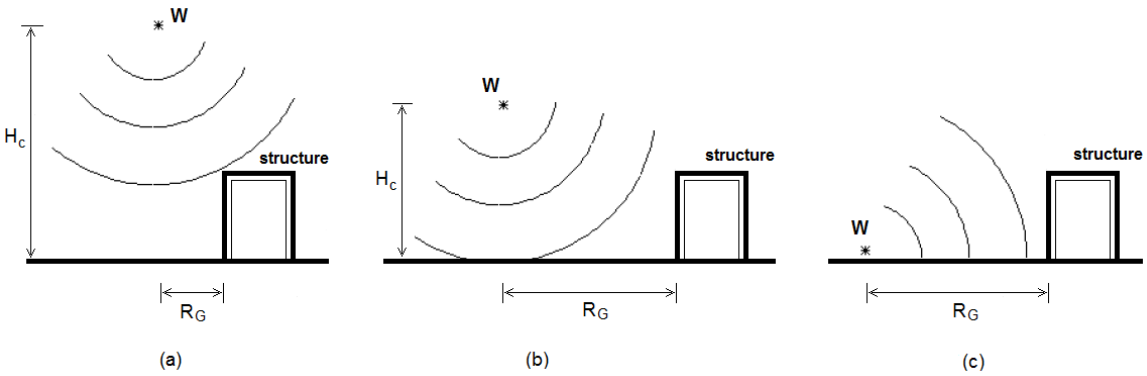

Figure 3: Types of external explosions and blast loadings; (a) Free-air bursts, (b) Air bursts, and (c) Surface bursts.

Associated to each of these explosion types is a characteristic blast loading of the structure, as reflections and interference phenomena along the propagation path can greatly modify the wave intensity and consequently the loading pressures. More practical information about this explosion and loading distinction will be provided in the following sections.

2.5 Blast wave reflection

The interaction between an object and a blast wave generates a pressure pattern which is different than the idealized time history presented in Figure 1. As the blast wave travels through space, decreasing in speed and peak pressure value, it encircles every object/structure that lies within its range. The load that has to be withstood by a structure depends on various parameters, such as the type and weight of the explosive charge, the distance of the detonation point, the structure's geometry and type, the interaction of the wave with the environment and the ground, etc.

When the blast wave comes to contact with a rigid surface the pressure that is reflected is larger than the incident peak pressure P_{so} shown at Figure 1. The reason for this rise is attributed to the nature of the propagation of the blast wave through the air. While the wave travels, it moves along air particles that collide with the surface upon arrival. In an ideal linear-elastic case the particles should be able to bounce back freely leading to a reflected pressure equal to the incident pressure, and thus the surface would experience a doubling of the acting pressure. In a strong blast wave, which as a shock wave is a non-linear phenomenon, the reflection of these particles is obstructed by subsequent air particles that are transferred there, thus leading to much higher reflected pressure values. In this case the surface would experience an acting pressure much higher than the incident one.

Clearly it is this reflected pressure to be used for design**.** Figure 4 shows the difference between the incident and the reflected pressure in an infinite surface. As just noted, the reflected pressure can be several times larger than the incident pressure, depending on the geometry of the structure, the type, size, weight and distance of the explosive as well as the interference of other obstacles between the detonation point and the structure. Figure 4 also depicts a typical ***dynamic pressure*** time history, which will be discussed extensively at section 2.8.

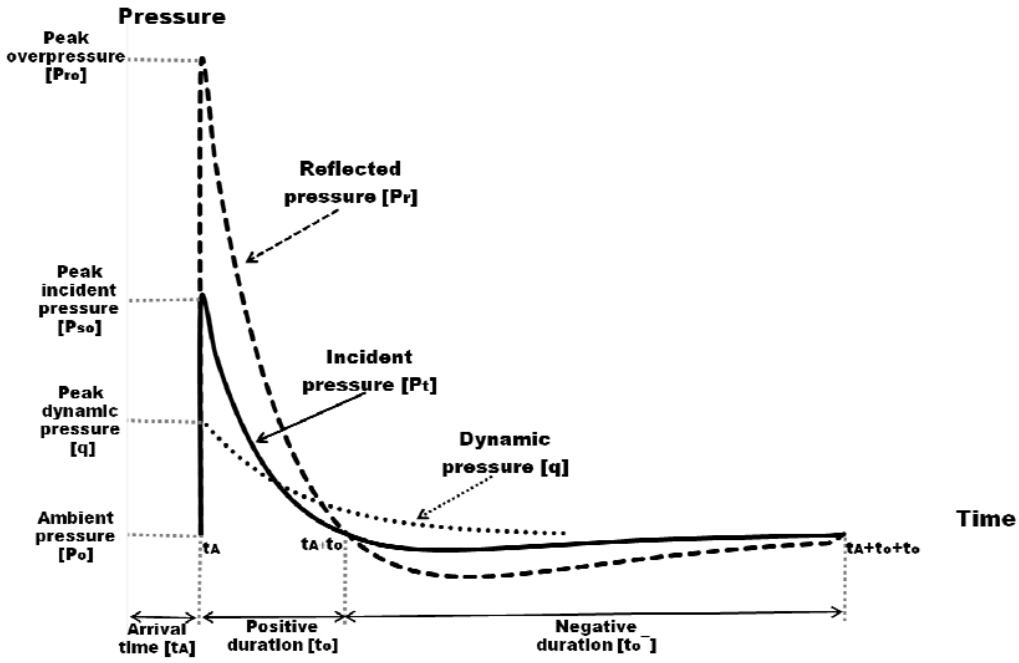

Figure 4: Incident, reflected and dynamic pressure time histories.

Three types of reflection can take place depending on the angle of the reflecting surface with the propagation direction of the blast wave. The most severe case, in terms of loading values, is when a surface is perpendicular to the direction of the wave, during which normal reflection occurs. When the propagation direction of the wave intersects at a small oblique angle with the surface it causes the creation of an oblique reflection, whereas the third case is linked to a phenomenon known as Mach stem creation, which occurs whenever the wave impinges on a surface at a specific angle, as will be explained below.

Clearly, in all cases the reflected pressure is always greater than the incident pressure. As mentioned earlier, the peak incident pressure is also referred to as the peak side-on overpressure because it is equal to the reflected pressure on a surface that is parallel to the direction of the blast wave. Figure 5 illustrates the difference between the reflected and the side-on overpressures in the case of a free air explosion without wave amplification. The value of the reflected pressure from the surface becomes maximum at the point of normal distance R_A between the detonation source and the surface. As expected, the reflected pressure's value decreases (however not monotonically!) as the angle of incidence α increases. Its minimum value is equal to the incident pressure and is created on surfaces perpendicular to the shock front ($\alpha = 90^o$).

Equation (6) can give the value of the peak reflected overpressure in the case of reflections at zero angle [2],

$$P_r = 2P_{so}\frac{4P_{so}+7P_o}{P_{so}+7P_o} \tag{6}$$

where, P_{so}= incident peak overpressure and
P_o= ambient pressure.

For this equation it was assumed that the explosion takes place at standard sea level conditions and that the ratio of specific heats of gases is equal to 1.4. According to Equation (6) the maximum and minimum reflected pressures could be obtained by letting $P_{so}\rightarrow\infty$ and $P_{so}\rightarrow 0$, respectively. This substitution leads to reflected pressures values ranging from 2 to 8 times the incident pressure for small and large shocks, respectively. Nevertheless, experimental investigations have concluded that the reflected pressure can be several times higher than 8 times the incident pressure. This is attributed to the fact that under severe blast loads the air does not behave in an ideal manner, which is an underlying assumption of Equation (6). It also indicates that the ratio of the normal maximum reflected pressure and the incident pressure is not constant, but depends on the value of the incident pressure.

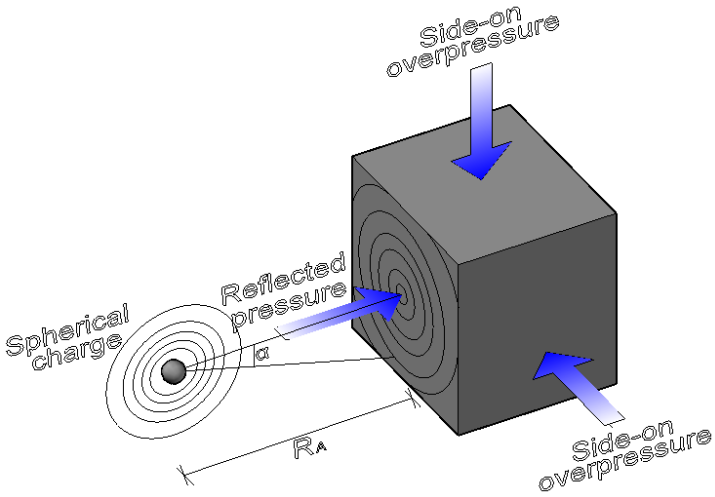

Figure 5: Definition of reflected pressures for a cube type structure.

As specified, Equation (6) is valid in the case of normal reflection. If there is an angle α (angle of incidence) between the wave propagation direction and the affected surface, the process of reflection may be quite different. This angle affects the resulting reflection and, consequently, the blast loading on a structure. Figure 6 shows the influence of the peak incident overpressure P_{so} on the peak reflected pressure $P_{r\alpha}$ versus the angle of incidence α, expressed in terms of the reflection coefficient $c_{r\alpha}$, which is defined as

$$c_{r\alpha} = \frac{P_{r\alpha}}{P_{so}} \tag{7}$$

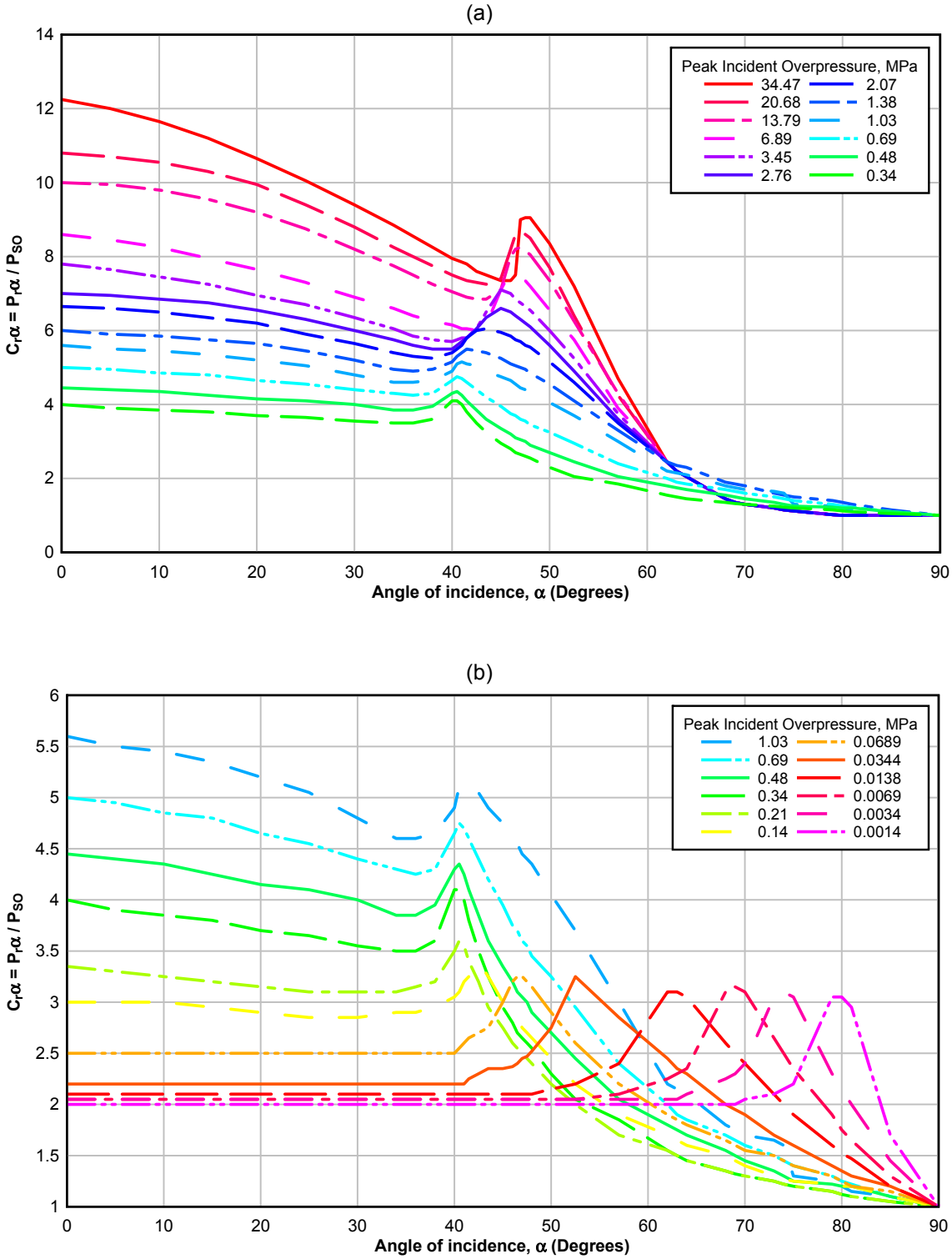

Figure 6: Influence of angle of incidence on the reflected pressure coefficient (a) for larger and (b) for smaller incident overpressure values (modified from [9]).

The effect of the angle of incidence may be neglected and the structure is studied under the normal reflected pressure, which is on the safe side for most cases, especially if the incident overpressure is large. More specifically, from the curves of the diagram it can be concluded that whenever the angle of incidence is approximately less than 40°, the use of the normal reflected pressure leads to conservative design as the normal reflected pressure is bigger (up to 25%). For small to moderate values of peak incident pressures (0.01-3.50 MPa) the reflected pressure at angles of incidence between 40°-55° can be underestimated if the assumption of a normal reflection has been made.

The reason for this reflected wave behaviour for angles of incidence between 40°-55° is attributed to the creation of a Mach stem. As already discussed, the blast wave due to an air detonation above the ground is made up of an incident wave, emanating from the explosive charge, and of a reflected wave, which is produced from the reversal due to the impingement of the wave to the ground. For shallow incident angles with the ground (up to 40°) the incident wave is ahead of the reflected wave produced by the surface and typical reflection occurs. For larger angles though, coalescence between the incident and the reflected wave takes place, as shown in Figure 7, creating a Mach stem. This coalescent wave can in some cases be substantially larger than the normal reflection pressure values, as was shown in Figure 6. The point of intersection of the incident, reflected and Mach waves is known as the triple point. The Mach stem is considered to have a constant value throughout its height, even though some small variations may exist.

In Figure 7 the case of an air burst is schematically examined where the blast wave is reflected from the ground before it hits the structure. The distance of the detonation point from the ground is much smaller than the distance from the obstacle (structure), thus leading to the creation of a Mach stem on the ground. The Mach front pressure-time history is similar to the incident pressure, depicted at Figure 1, but its value is larger. From Figure 7 it can also be observed that the height of the Mach front, (triple point), increases with increasing propagation distance.

This results in situations where structures:

i) can either be loaded by uniform pressure, if the Mach front height is larger than the height of the structure, or
ii) can be loaded uniformly by the Mach front over their lower part (bellow triple point) and by the separate action of the incident and reflected pressures over their upper part (above triple point).

The corresponding incident overpressure profiles are schematically shown in the middle part of Figure 7. Of course, for design purposes this second loading case can be substituted by applying the uniform pressure of the Mach front (whose value is larger) all-over the structure's height. Design manuals such as [8-9] contain diagrams for the calculation of the Mach pressure, impulse and height according to the distance and weight of the blast charge from the structure under study. At the bottom part of Figure 7 a diagram for the calculation of the triple point's height is presented.

Similar to Figure 6 for $P_{r\alpha}$, the peak reflected impulse values $i_{r\alpha}$, when the angle of incidence is greater than 0^0, can be conveniently calculated and used. The relevant curves, which are strictly valid for free-air bursts and spherical waves, are shown in Figure 8a and 8b.

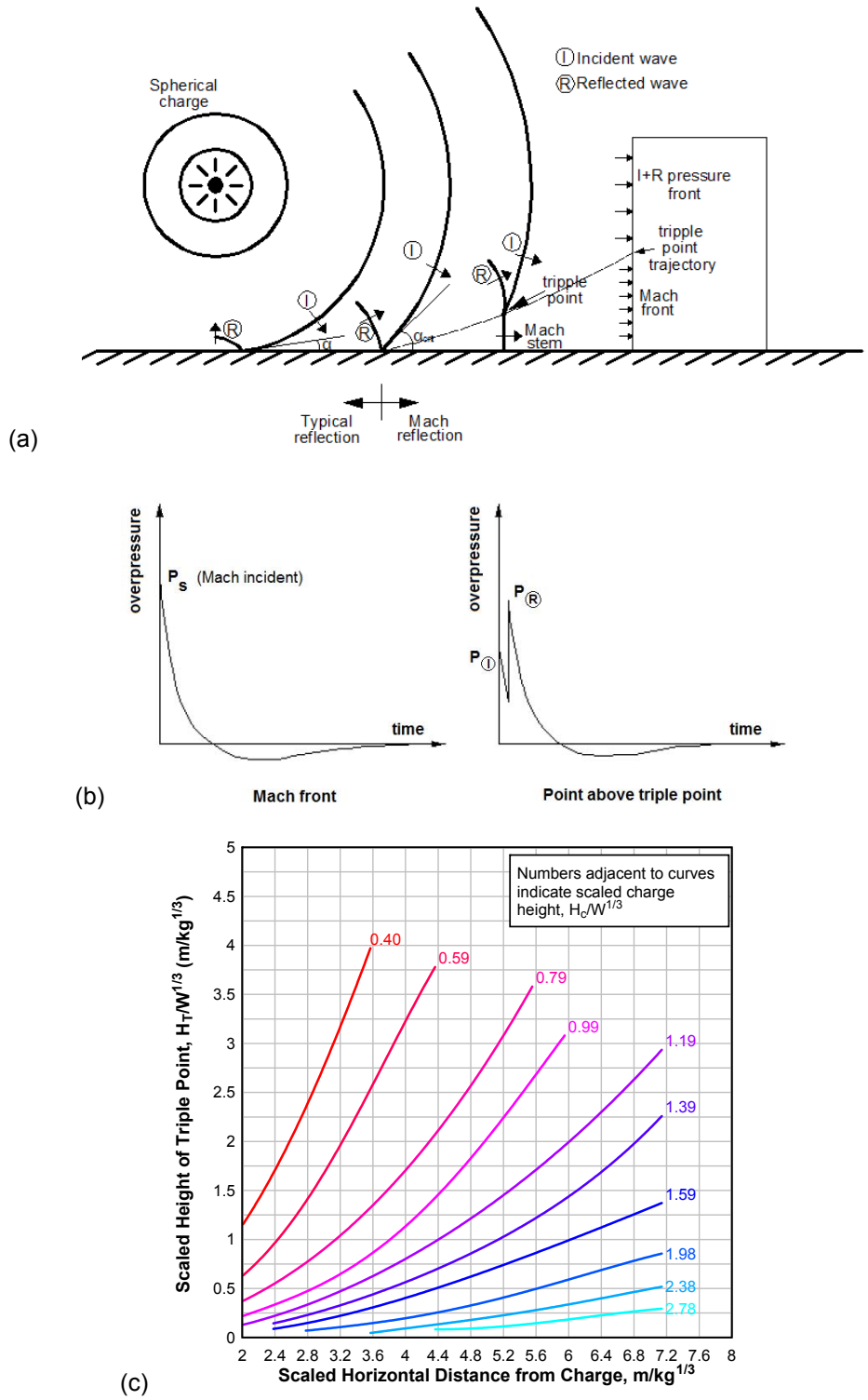

Figure 7: (a) Mach stem creation over a horizontal (ground) surface and loading of a vertical surface; (b) profile of incident overpressure within the Mach front height, and of that above the triple point, respectively; (c) estimation of Mach front height H_T from the scaled charge height $H_c/W^{1/3}$ and scaled horizontal distance $H_G/W^{1/3}$.

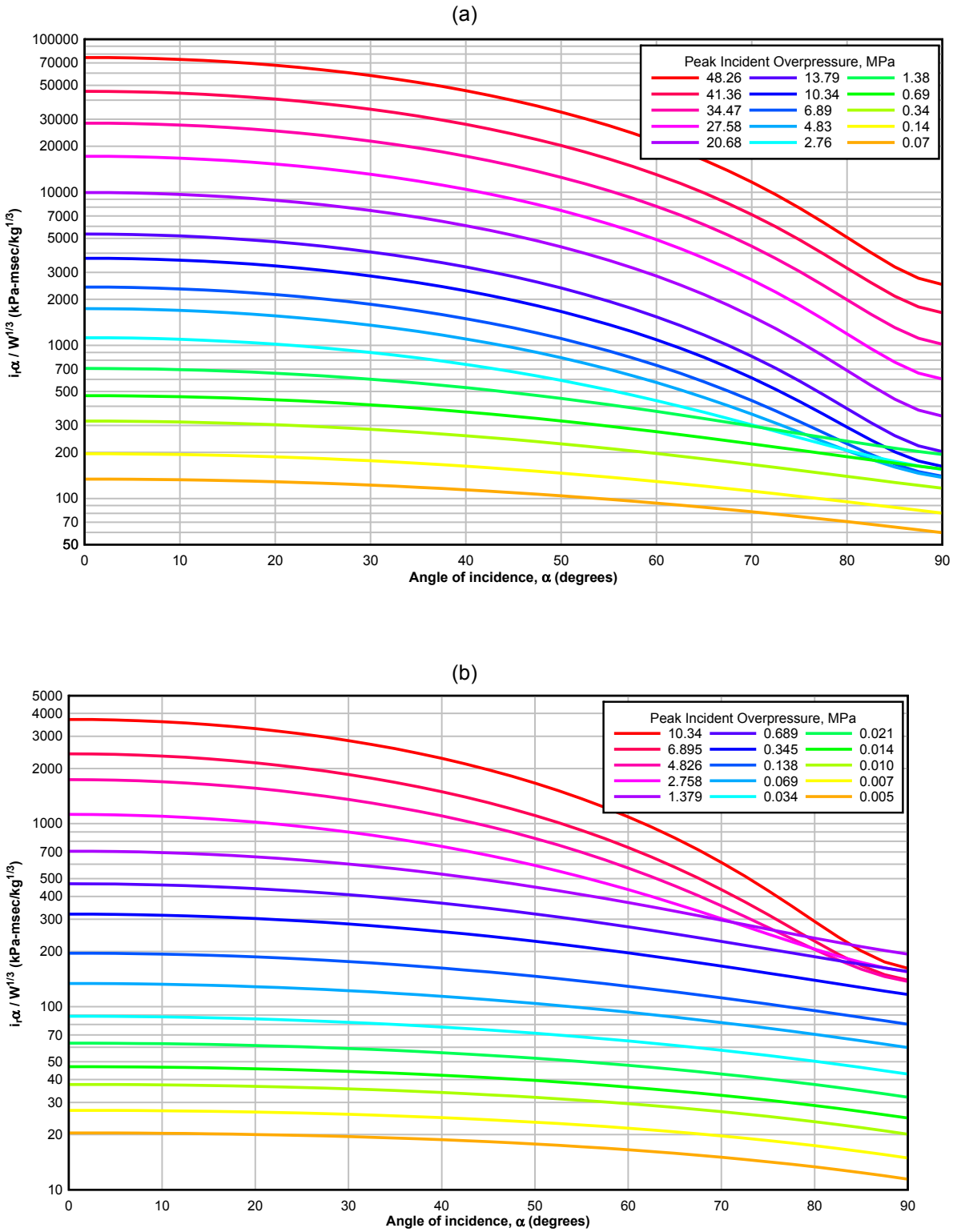

Figure 8: Influence of angle of incidence on the scaled reflected impulse for (a) larger-value incident pressures and (b) lower-value incident overpressures (modified from [9]).

2.6 Surface burst and loading

A common case for a terrorist attack bombing scenario is the use of a vehicle loaded with explosives that is detonated by using a remote control or time trigger. What is special about this type of explosion, which is of practical importance for designers, is the fact that due to the closeness to the ground there is an immediate interaction between the ground and the blast wave. This is the so-called hemispherical surface burst. Instead of the creation of a Mach front at a certain distance from the point of blast initiation, the incident wave is reflected immediately from the ground leading to higher pressure values.

If the ground were a rigid surface, the generated pressure would be twice that produced by the same charge under free-air burst conditions. This observation allows the use of the pressure relationships derived for free-air blasts also in the case of surface bombings, by doubling the original charge weight. In reality, depending on the soil and explosive type [7], some kind of energy absorption takes place from the ground by the creation of a crater, and thus the multiplicative factor applied to the charge is approximately 1.7 to 1.8. The generated wave has a hemispherical shape, as shown in Figure 9, and its characteristics resemble those of the Mach front wave that was described earlier. For a sufficient large stand-off distance this wave can be considered locally as plane, and the pressure loading of a structure can, for practical purposes, be considered as uniform.

In Figure 8 apart from the pressure on the front side, the pressures applied at the top of the structure are also schematically shown. When the blast wave comes to contact with an obstacle it eventually engulfs it, thus exerting pressures to all of its exposed sides. In the case of a stand-alone building the blast wave first hits its front face and subsequently it diffracts around the rest of the structure, loading the roof, the side and the rear walls. As was pointed out earlier, the roof and the side walls are parallel to the blast wave propagation direction, which means that they are loaded according to the incident pressure, (with a reduction due to the negative drag pressure).

In order to calculate the pressure to be applied at the side walls and the top of the structure a procedure is proposed in [8-9] which is based on an equivalent load factor C_E and a drag coefficient C_D (as will be explained in Chapter 3). These factors are computed as functions of the wavelength and essentially they average the applied non-uniform pressure over the length of the surface. In case that the side walls are not parallel but at an angle to the blast wave propagation direction, the procedure proposed for the front walls should be adopted.

Concerning the rear wall, as the pressure wave passes the edges of the side walls and the roof, secondary waves are created which are responsible for loading the back of the structure. For design purposes the calculation of the pressures acting at the rear wall is essential for the determination of the overall drag force acting on the structure. Usually the same formulation used for the side walls and the roof is applied, and involves the peak pressure value acting at the back edge of the roof slab, as will be shown below.

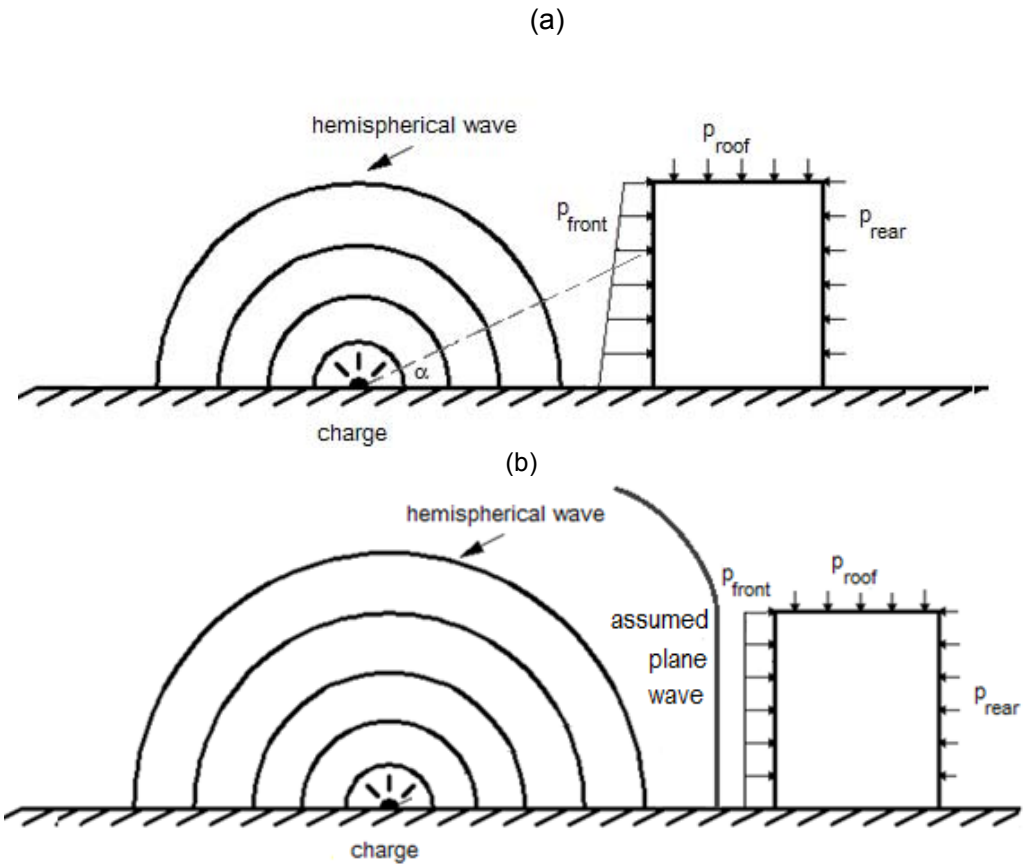

Figure 9: Pressure acting on a building due a surface burst (a) at a close distance, (b) at a distance sufficient for the impinging wave to be considered as plane.

2.7 Effect of finite reflecting surface

The reflected curve shape shown in Figure 4 is valid in the case of a blast wave acting on an infinite surface. For a single building though, the reflected pressure from the front of the structure is eventually relieved by the leakage of the wave around its sides and roof regardless of the type of blast (surface burst or free-air). This phenomenon allows the reflected pressure to be reduced at a fast rate and finally to become equal to the sum of the side-on and the dynamic pressure. The time required for the reflected pressure to drop to this lower level is known as clearing time t_C.

Figure 10 depicts the difference between the reflected pressure curves in the case of a finite and an infinite surface. The peak reflected pressure is identical for both cases, but the curves follow a different path during their decay part. The clearing time is also shown according to the definition presented above. The positive phase duration in the case of a finite surface is generally smaller than an infinite one, as in the former the pressure values drop faster due to the wave's propagation over the sides/roof of the surface. The immediate impact of this effect is the reduced total force at the surface of the obstacle since the impulse, which is computed as the integral of the pressure-time diagram, is considerably smaller. As will be seen below, the clearing time is not only dependent on the geometry of

the obstacle, but also on the charge type and weight and the detonation point's distance from the building (stand-off distance).

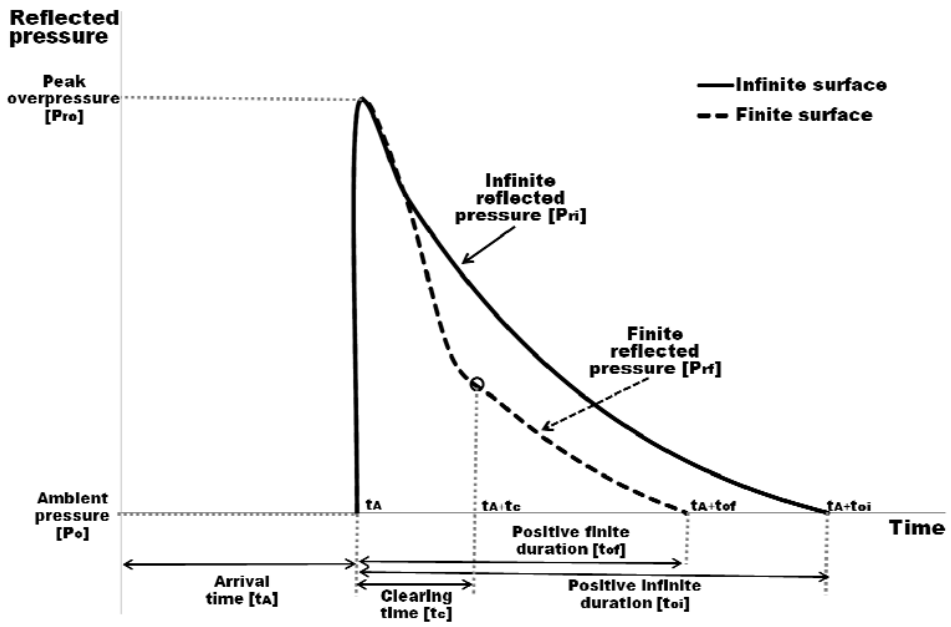

Figure 10: Influence of surface's finite dimensions on the reflected pressure time-history.

2.8 Dynamic pressure

The blast wave propagates through the air with a continuously decreasing speed which is larger than the speed of sound. The air behind the front of the blast wave moves also along the same direction as a wind but with smaller velocity. These winds behind the blast wave front are responsible for loading a surface for the whole duration of the positive phase and also for a small time afterwards. The pressure that is produced is known as **dynamic** or **drag pressure *q*(t)**, it has an initial peak value q_o, which is less than that of the incident or reflected pressures for medium and small overpressure values, and it eventually dies out. The difference is that both incident and reflected pressures last only for a very short time (usually far less than one second), while the dynamic pressure may last for longer periods (up to 2-3 seconds).

Figure 11 shows the variation of the peak dynamic pressure as a function of peak incident pressure values. The dynamic pressure depends on the density of the air and the wind velocity behind the front of the blast wave, all of which are influenced by the peak incident overpressure. Its effective value further depends, through a drag coefficient, on the orientation of the surface with respect to the blast wind direction, as will be presented in more detail in Section 3.2.

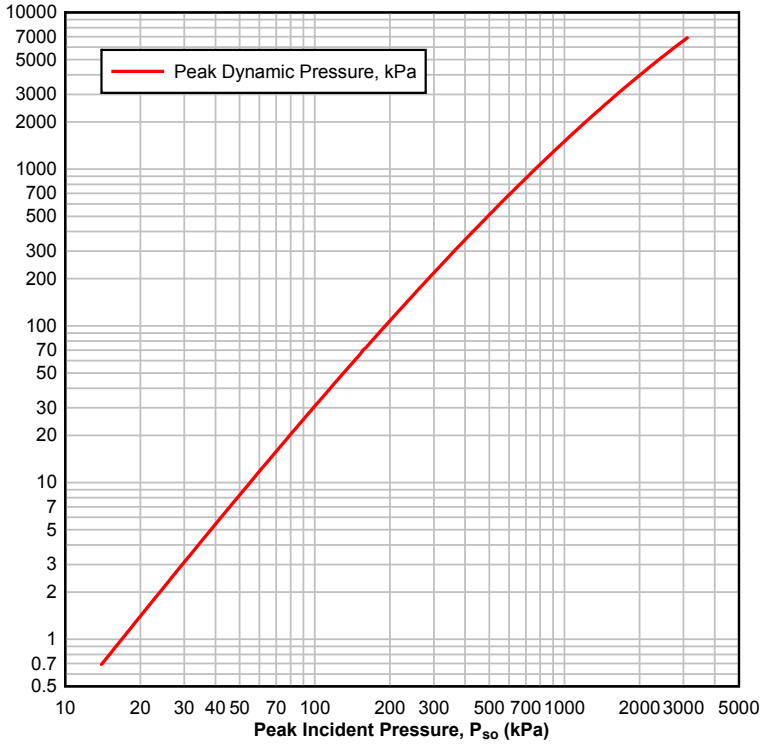

Figure 11: Variation of peak dynamic pressure q_o versus peak incident pressure (modified from [9]).

3. Calculation of structural blast loads

3.1 Blast pressure determination

There are various relationships and approaches for determining the incident pressure value at a specific distance from an explosion. All the proposed relationships entail computation of the scaled distance, which depends on the explosive mass and the actual distance from the center of the spherical explosion.

Kinney [3] presents a formulation that is based on chemical type explosions. It is described by Equation (8) and has been used extensively for computer calculation purposes,

$$P_{so} = P_o \frac{808\left[1+\left(\frac{Z}{4.5}\right)^2\right]}{\left\{\left[1+\left(\frac{Z}{0.048}\right)^2\right]\left[1+\left(\frac{Z}{0.32}\right)^2\right]\left[1+\left(\frac{Z}{1.35}\right)^2\right]\right\}^{0.5}} \tag{8}$$

where Z (m/kg$^{1/3}$) is the scaled distance, Equation (4), and P_o is the ambient pressure.

Other relationships for the peak overpressure for spherical blast include those of Brode [11], shown in Equations (9). They depend on the magnitude of the explosion, Equation (9a) is valid where the peak overpressure is over 10bar (=1MPa) (near field explosions) and Equation (9b) for pressure values between 0.1 bar and 10 bar (0.01MPa-1MPa) (medium and far-field explosions). The scaled distance is measured in m/kg$^{1/3}$ and the pressure P_{so} in bars,

$$P_{so} = \begin{cases} \dfrac{6.7}{Z^3} + 1 & , for \quad P_{so} > 10\, bar \\ \dfrac{0.975}{Z} + \dfrac{1.455}{Z^2} + \dfrac{5.85}{Z^3} - 0.019 & , for \quad 0.1 < P_{so} < 10\, bar \end{cases} \tag{9}$$

Another formulation, that is widely used for computing peak overpressure values for ground surface blast has been proposed by Newmark [12] and does not contain categorization according to severity of the detonation:

$$P_{so} = 6784 \frac{W}{R^3} + 93 \sqrt{\frac{W}{R^3}} \tag{10}$$

where, P_{so} is in bars,

W is the charge mass in metric tons (=1000kg) of TNT and

R is the distance of the surface from the center of a spherical explosion in *m*.

Mills [13] have also introduced an expression of the peak overpressure in kPa, in which W is expressed in kg of TNT and the scaled distance Z is in m/kg$^{1/3}$, which reads:

$$P_{so} = \frac{1772}{Z^3} - \frac{114}{Z^2} + \frac{108}{Z} \tag{11}$$

The most widely used and accepted approach for the determination of blast parameters is the one proposed by Kingery-Bulmash [7]. Their paper includes formulations for both spherical (free air bursts) and hemispherical pressure waves (surface bursts) and provide the values of incident and reflected pressures as well as of all other parameters. The proposed blast parameters are valid for distances from 0.05 m to 40 m as the diagrams included in [7] are referred to 1kg of TNT.

For comparison purposes Figure 12 compiles the curves of the above expressions for peak incident overpressure versus scaled distance for both free-air bursts (spherical waves) and surface bursts (hemispherical waves). The corresponding curves of the Kingery-Bulmash study are included for reference. It is observed that the curves of Equations (9), (10) and (11) substantially deviate from the Kingery-Bulmash ones for small scaled distances. This may be due to the fact that these equations were developed principally for nuclear blasts and not for conventional explosives. The Kinney curve, Equation (8), yields satisfactory predictions over the whole scaled distance range.

As is widely recognized in the engineering practice [8-10], the Kingery-Bulmash curves are employed as the standard throughout this work.

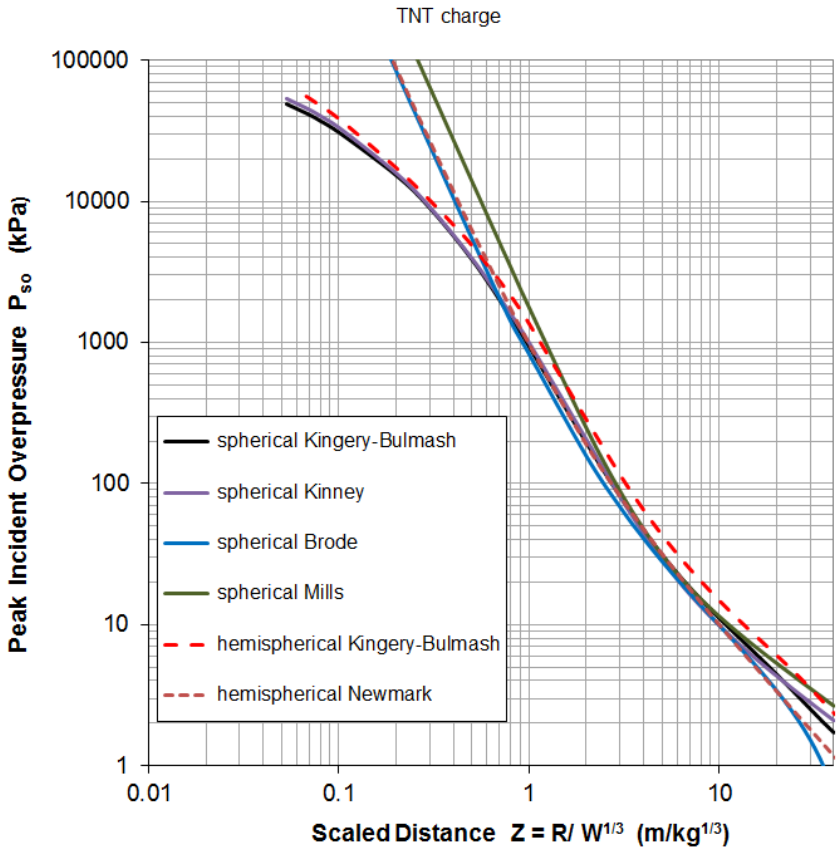

Figure 12: Comparison of curves of peak incident overpressure versus scaled distance for both free-air bursts (spherical waves) and surface bursts (hemispherical waves).

Reference [7] also includes a full set of analytical relationships providing the above blast parameters in terms of polynomial functions of the logarithm of the scaled distance. These relationships can be readily programmed and Figures 13 and 14 show the diagrams of blast parameters for the positive phase of the blast wave for both free-air and surface bursts. These diagrams are the metric-units rendition of the curves contained in references [8] and [9]. They are overall more comprehensive and the curves have been drawn with respect to scaled distances from Z=0.05 m/kg$^{1/3}$ to Z=40 m/kg$^{1/3}$. From these diagrams in order to obtain the absolute value of each parameter, its scaled value has to be multiplied by a factor $W^{1/3}$ so as to take into account the actual size of the charge. Clearly, as mentioned above for the Hopkinson-Cranz scaling law, pressure and velocity quantities are not scaled.

Most of the symbols encountered in Figures 13, 14 and 15 have been defined in Figure 1, where the idealized pressure-time variation curve is shown. The additional symbols stand for: U= shock wave speed (m/ms) and L_w= blast wavelength (m). This latter can be defined, for a point at a given standoff distance at a particular time instant, for L_w^+ as the length which experiences positive pressure (or, negative pressure for L_w^-).

Figure 15 shows the diagrams for blast parameters of the negative phase of the blast wave for both free-air and surface bursts for TNT charges at sea level, as adapted from [8]. These

parameters are important if the behaviour of the structure to the whole blast phenomenon is necessary.

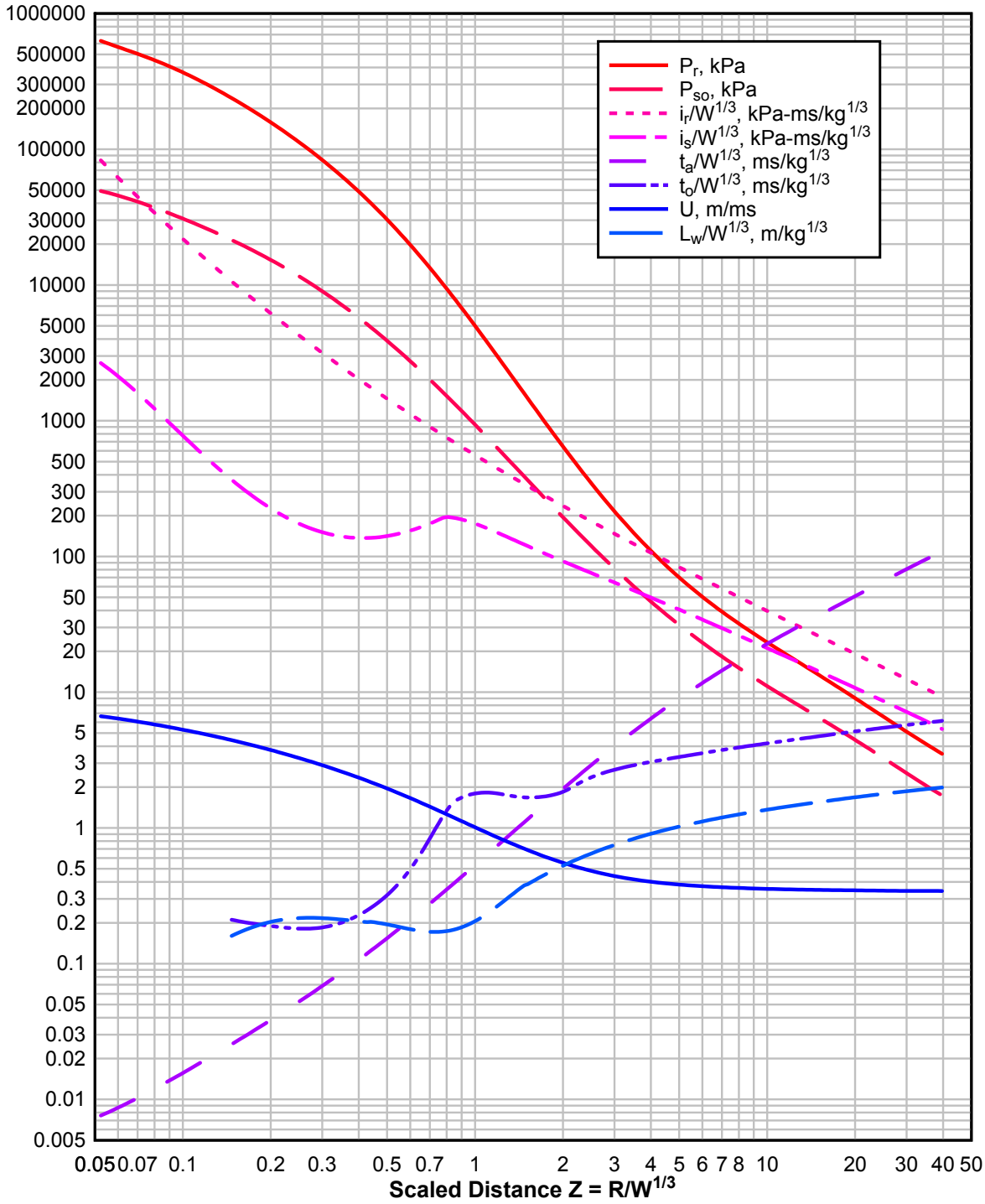

Figure 13: Parameters of positive phase of shock spherical wave of TNT charges from free-air bursts (modified from [9]).

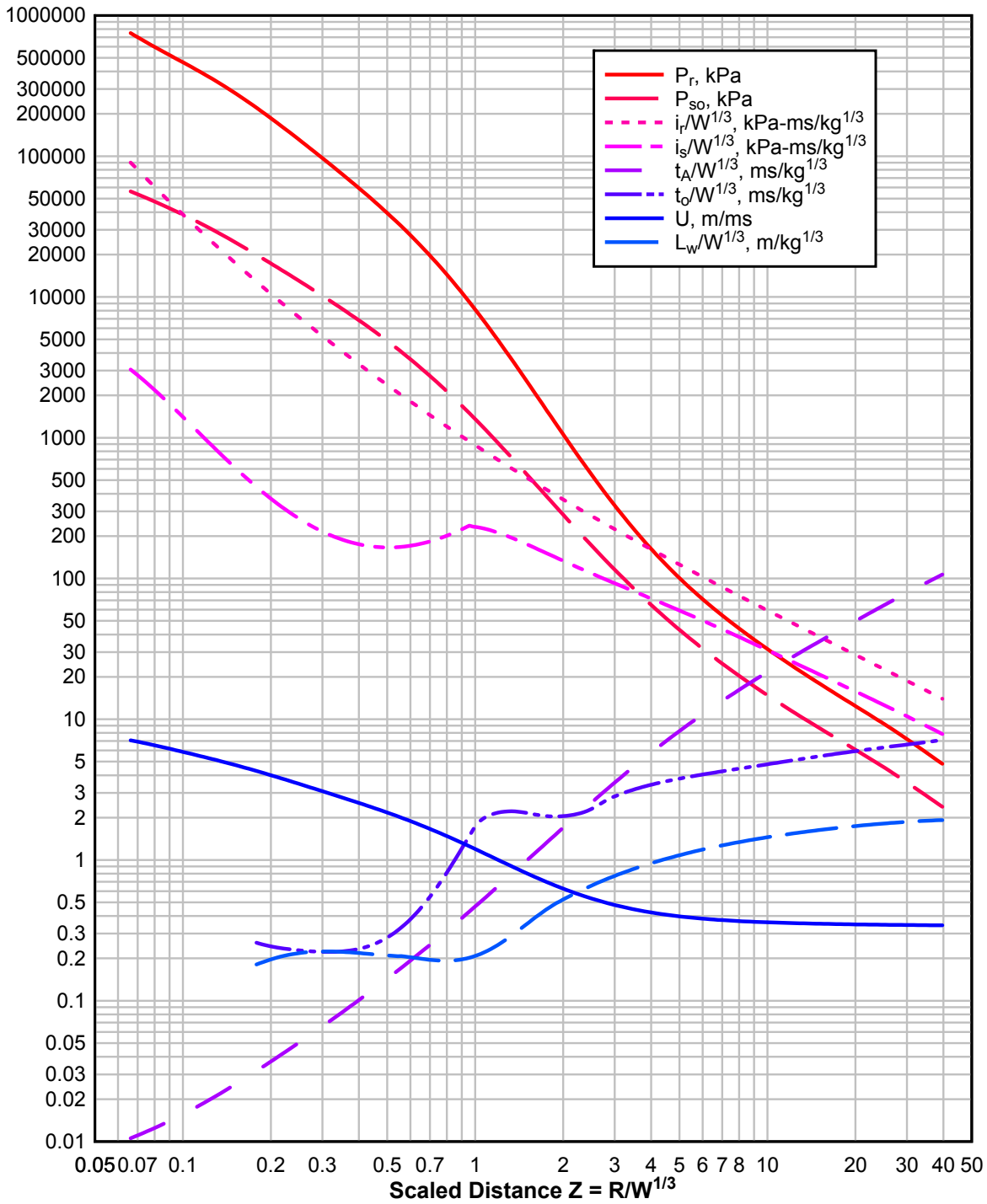

Figure 14: Parameters of positive phase of shock hemispherical wave of TNT charges from surface bursts (modified from [9]).

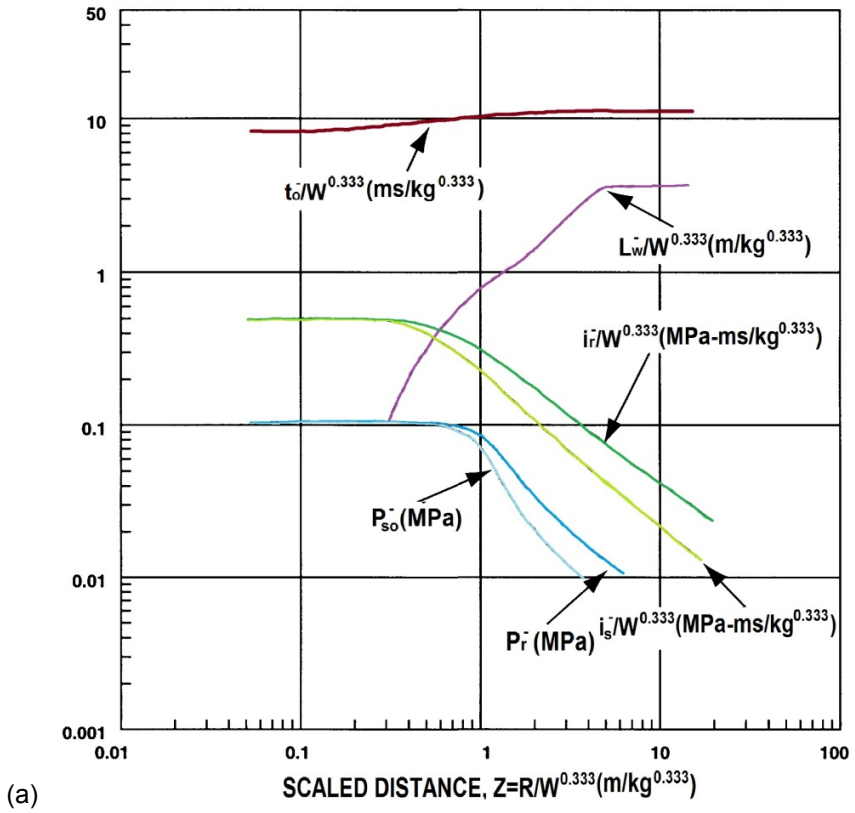

(a)

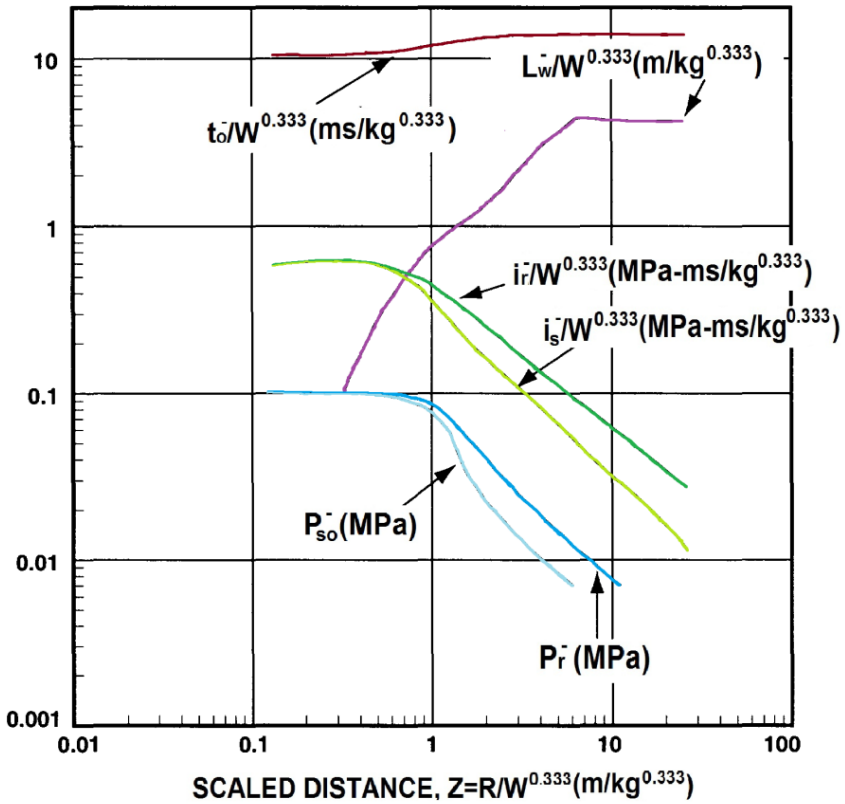

(b)

Figure 15: Parameters of negative phase of shock wave of TNT charges, (a) from spherical free-air bursts, (b) from semispherical surface bursts (modified from [9]).

3.2 Calculation of pressure loads on building surfaces

3.2.1 Blast wave-structure interaction

A structure subjected to an external explosion will eventually be engulfed by the blast wave and normal forces (pressures) will be applied to its exposed surfaces. The above sections described the basic characteristics of a blast wave and the way to calculate important values for design, such as its peak incident and reflected pressures. Apart from these values, the response of a structure under explosion loading depends also on various other factors such as the shape of the structure, the relative location of the blast from the structure, the geometry of the area between the structure and the detonation point, the natural period of the structure, its openings etc.

The fundamental (or equivalent, if a single-degree-of-freedom is considered) natural period T_n of the structure and its relation to the positive phase duration t_o of an excitation play an important role on its behaviour. If the duration of the excitation is longer than the natural period T_n of the structure, then its maximum deflection takes place before the excitation ceases, and dynamic analysis should be used, as often is the case for earthquake loading. If the duration of the positive phase of the excitation is a lot shorter than the natural period ($<T_n/4$) of the structure, then one deals with an impulsive loading. For a particular structure and load type (e.g. pressure), these considerations can be schematically depicted, as in Figure 16, by an iso-response curve in a so-called pressure-impulse (P-I) diagram. Thus, for very short duration loads (relative to T_n) the structural response is sensitive to the associated impulse and not to the maximum pressure (vertical asymptote). However, as the load duration increases to quasi-static, the response starts becoming sensitive to the maximum value of pressure and not to impulse (horizontal asymptote).

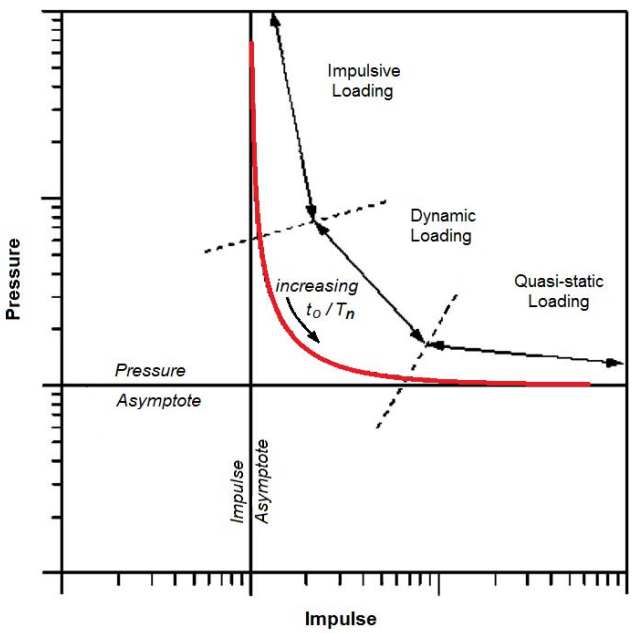

Figure 16: Sketch of a typical Pressure-Impulse diagram.

The majority of the structures has a natural period that is far greater than the duration of the positive phase of the blast wave, which is of the order of milliseconds. These structures barely experience a deflection before the complete passage of the blast wave, so they are loaded according to the impulse value of the wave's time history. For this reason these structures are usually considered as rigid throughout the positive and negative phase of a blast wave and the analysis can be performed as decoupled. This means that the structural response is calculated without considering the interaction between the blast pressure loading and the deforming structure.

3.2.2 Pressure on the front wall

The first surface that will be loaded from the blast wave is the building's front façade. In TM5-1300 [8] a procedure is proposed for the calculation of the load that has to be sustained by the front face, but an assumption is made that the loaded face is within the region of the Mach stem whose height exceeds the total height of the building. For surface bursts this means that the detonation point is situated at such a distance from the structure that the blast wave front can be considered as plane. The first step for the definition of the total impulse applied to the front face of the building is the calculation of the peak reflected pressure P_r at time $t=t_A$ when the blast wave arrives at the surface. The reflected pressure is related to the incident pressure as was shown at Figure 6. As commented in section 2.7, the pressure at the front face starts decreasing as the wave moves past the surface surrounding the rest of the structure within the clearing time t_C. At time t_A+t_C the pressure at the front surface will be substantially dropped (but still remaining higher than the initial ambient pressure). After time t_A+t_C the pressure is the result of the combined effect of the incident and the dynamic pressure and is provided by Equation (12),

$$P = P_s + C_D q \tag{12}$$

where, P_s is the incident pressure,
C_D is the drag coefficient, taken equal to C_D =1 for the front wall, and
q is the dynamic pressure.

As mentioned above, t_C is known as the clearing time and various formulations exist for its calculation. According to [8] it can be estimated by Equation (13).

$$t_C = \frac{4S}{(1+R)C_r} \tag{13}$$

where, S is the smallest of the surface's height H or half width $W/2$ (see Figure 19),
C_r is the sound velocity in the reflected medium, shown in Figure 17, and
R is the ratio of S/G, where G is the largest of the surface's height H or the half width $W/2$.

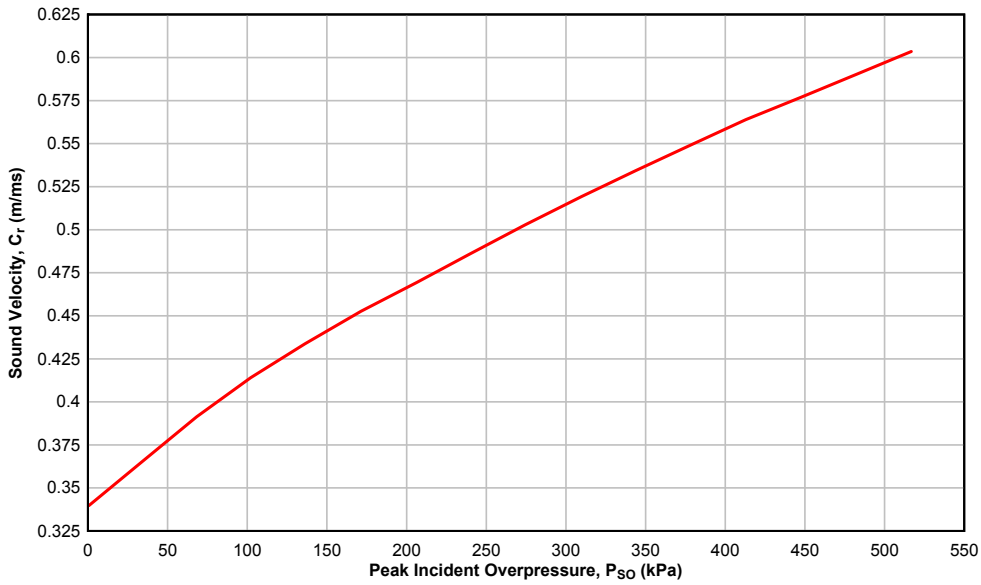

Figure 17: Sound velocity in reflected overpressure region (modified from [9]).

After the time t_A+t_C the pressure values at the front face of the structure continue to decrease to finally reach the value of the ambient pressure. In reality the form of this decreasing curve is practically exponential (Figure 10), as has already been discussed during the description of the ideal blast wave characteristics. In order to simplify the analysis the decrease of the incident and the dynamic pressure can be assumed to be linear and of triangular shape.

According to this approach the actual duration t_o of the positive phase of the incident wave is replaced by a fictitious time t_{of} ($t_{of} < t_o$) that depends on the positive impulse and peak pressure, as described by Equation (14).

$$t_{of} = \frac{2i_s}{P_{so}} \tag{14}$$

where, i_s is the impulse value of the positive phase of the blast wave and
P_{so} is the peak incident pressure.

A similar procedure can be applied for the negative phase of the blast wave thus defining a fictitious time t_{of}^- by employing the corresponding impulse and peak pressure values. The introduction of the fictitious time to produce simpler triangular pulses results in a time gap between the end of the assumed positive phase and the beginning of the negative, as can be seen at Figures 18 and 19.

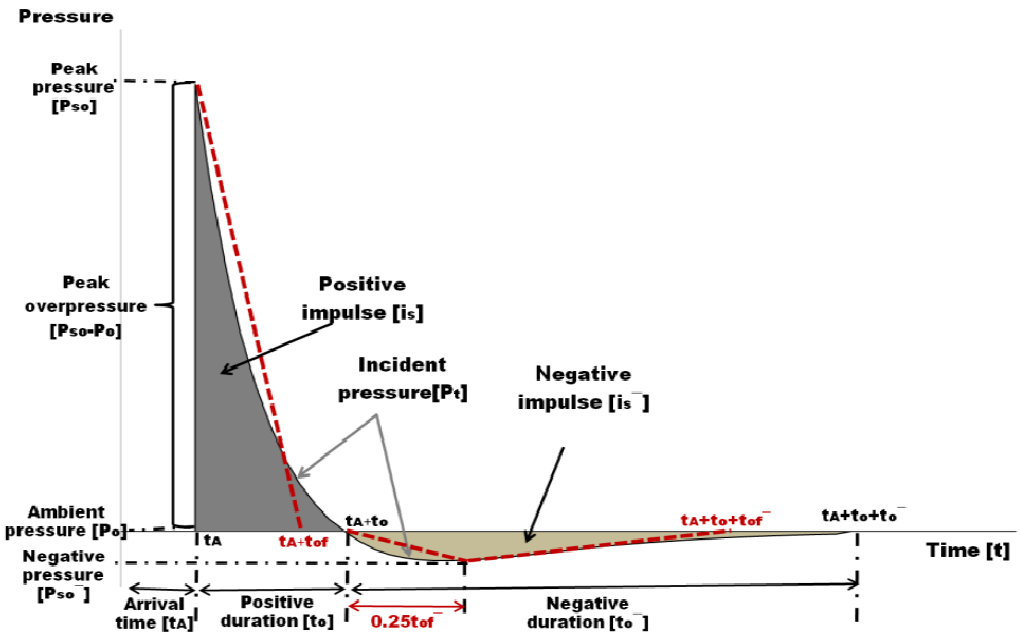

Figure 18: Substitution of actual incident pressure curve by triangular pulses and definition of relevant fictitious times.

The triangular shape assumption of the blast wave time history is not always accurate, especially whenever high pressure values are involved. From Equation (13) it is deduced that computation of the clearing time depends on the geometry of the impinged surface and the sound velocity in the reflected region, which in turn depends on the amplitude of the incident wave and not on the intensity of the explosion. Experiments have shown that whenever high pressure values are present, the positive phase duration of the blast wave is extremely short, resulting in a fictitious time t_{of} that is shorter than the clearing time t_c. In this case the aforementioned procedure will result in a triangular diagram that will not represent the true reflected pressure time history. The fact that the clearing time will not occur means that the reflected wave pressure time history should correspond to that applied on an infinite surface. For this reason an additional curve is usually constructed, as shown at Figure 19, which uses the total reflected pressure impulse i_r assuming a normal reflection. For a given P_{so} the reflected impulse i_r can be derived from the diagrams of Figures 13-14 and the fictitious duration t_{rf} for the reflected wave is computed through Equation (15).

$$t_{rf} = \frac{2i_r}{P_r} \tag{15}$$

where, i_r is the total reflected impulse and
P_r is the peak reflected pressure.

Thus for the positive phase of the reflected pressure two curves P_r*-t are* constructed and compared: one corresponding to infinite surface conditions, and another derived using the assumption that the finite surface geometry influences the value of the reflected pressure. The curve to be used for loading the structure is the one that produces the smallest impulse value.

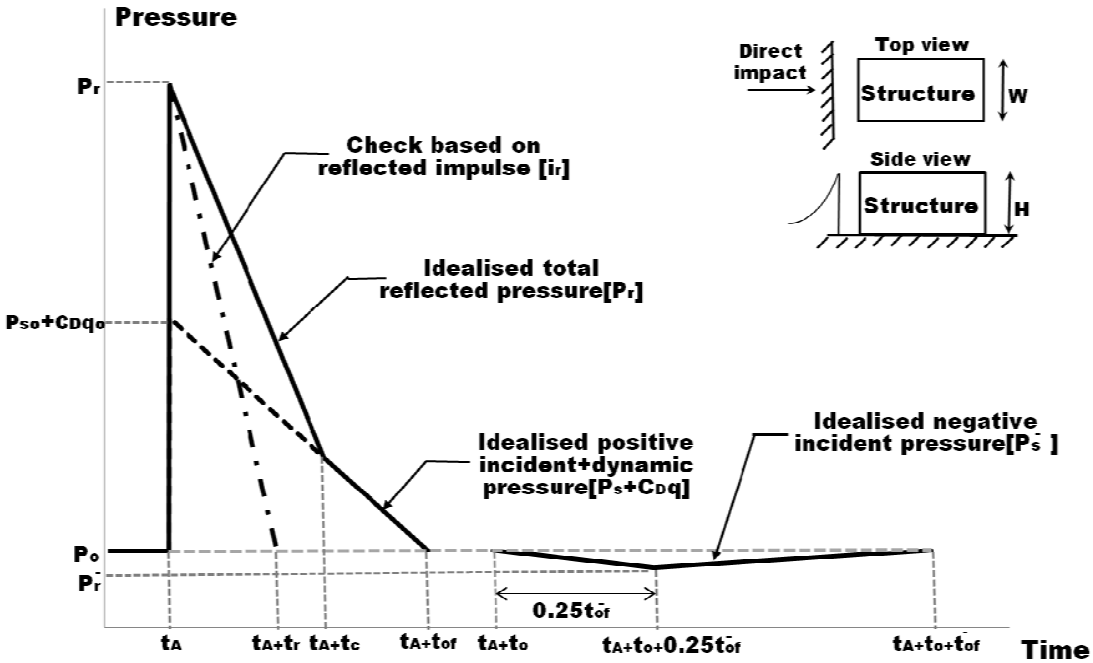

Figure 19: Triangular assumption of pressure time history on the front face of a structure.

3.2.3 Pressure on the roof and the side walls

The front face of a structure is loaded first as a consequence of a direct blast wave that impinges on it. As the wave propagates it surrounds the structure causing pressure rises at the roof, the side faces and the back surface. As has already been pointed out, if the side walls and the roof of the structure are parallel to the direction of the blast wave, they experience peak side-on overpressures that are equal to the incident pressure. Complex phenomena take place, like the differentiation of pressure values between the front and the back of the roof or the side wall surfaces, which initiate as a result of the wave flow around the edges of the front face. Usually these details are neglected in the design and a uniform, time-varying equivalent pressure is applied, whose peak value P_R is given by Equation (16).

$$P_R = C_E P_{sof} + C_D q_{of} \tag{16}$$

where, P_{sof} is the incident pressure at point *f* of the *front* edge of the roof, Figure 20,
C_E is the equivalent load factor,
C_D is the drag coefficient and
q_{of} is the dynamic pressure corresponding to $C_E P_{sof}$.

It is noted that the diffraction which takes place when the wave surpasses the edges of the front face, results in diminishing the side-on overpressure or under-pressure values. This is taken into account in [8] by the introduction of an equivalency factor C_E, which reduces the load acting on the surface and depends on the ratio of the blast wavelength to the length of the span of the surface (L_w/L in Figure 21).

The wavelength L_{wf} to be used in the following figures corresponds to that of point *f* (front edge of the roof), where the incident overpressure is P_{sof}; L_{wf} can be determined from the

diagrams of Figures 13-14. Figure 21 shows the equivalent load factor C_E as a function of the wavelength L_{wf} for both the positive and the negative phases of the blast loading. The peak pressure value for the roof P_R, as computed through Equation (16), also includes the (negative) contribution of the dynamic pressure. The drag coefficient depends on the severity of the blast and in particular of the peak dynamic pressure. Table 4 shows recommended drag coefficient values for the reported peak dynamic ranges [8].

Table 4: Drag coefficient C_D values for roof and side walls according to [8].

Peak dynamic pressure [kPa]	Drag coefficient
0-170	-0.40
170-350	-0.30
350-900	-0.20

Figure 20 shows the constructed pressure curve to be applied to the roof and the side walls of a structure due to blast loading. The load rises linearly to its peak value in time t_d, determined from the diagram of Figure 22 [8]. The pressures are averaged over the entire span length, so a uniform rise time to the peak positive or negative pressure can be used. The entire duration of both the positive and negative phase of the blast load can be calculated through Figure 23. The parameter t_{of} appearing in Figures 20 and 23 should not be confused with that of Figures 18, 19 etc.

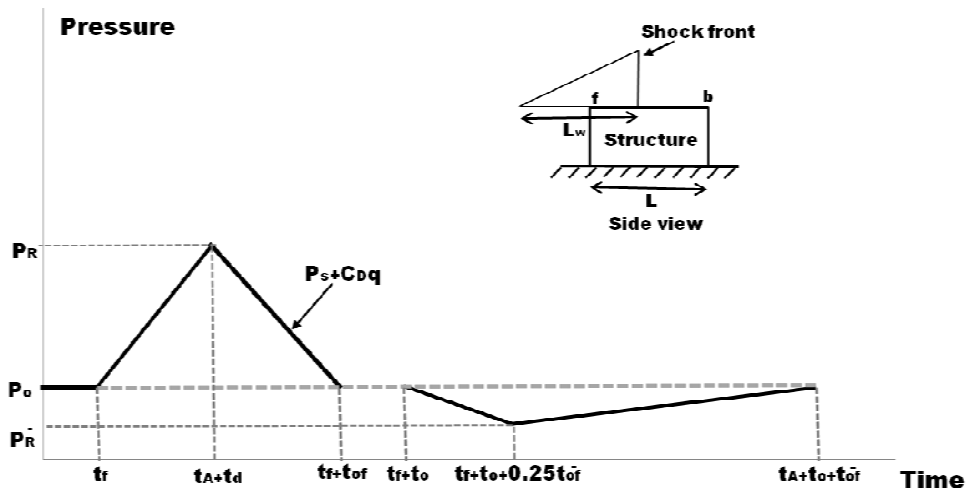

Figure 20: Idealized roof and side wall pressure-time variation, P_R=P_{Roof}.

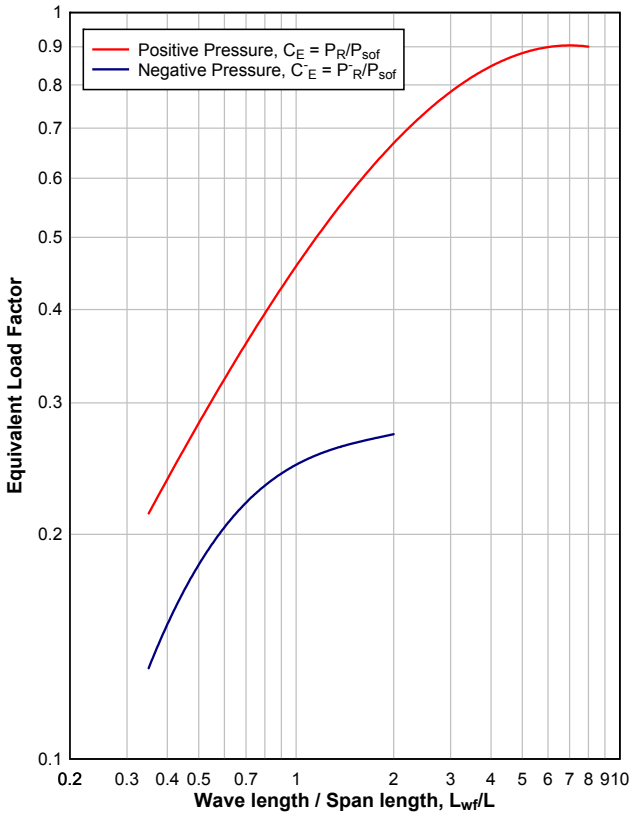

Figure 21: Load factors for positive and negative phase of blast loading for the roof and side-walls of a structure (modified from [9]).

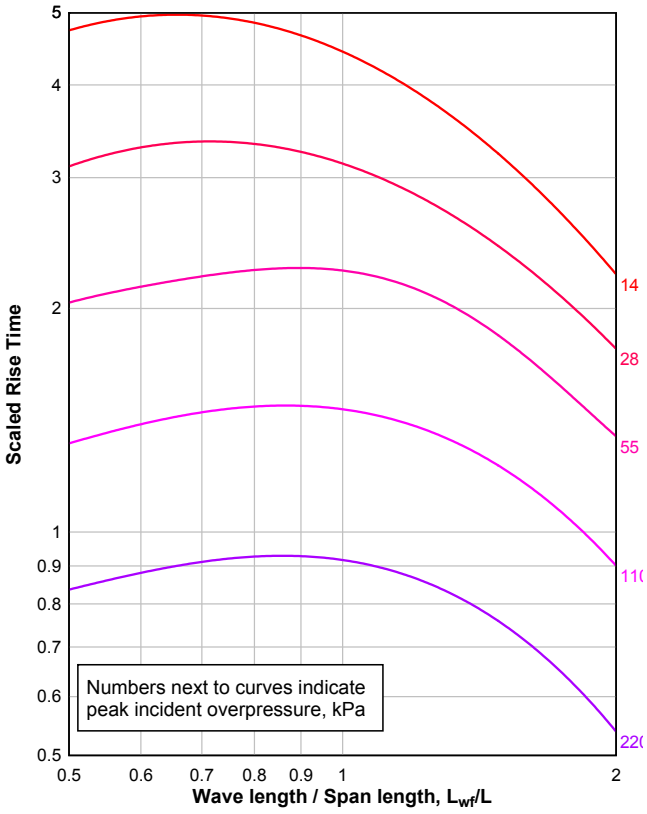

Figure 22: Scaled rise time t_d of positive and negative phase pressure loading for the roof and side-walls of a structure (modified from [9]).

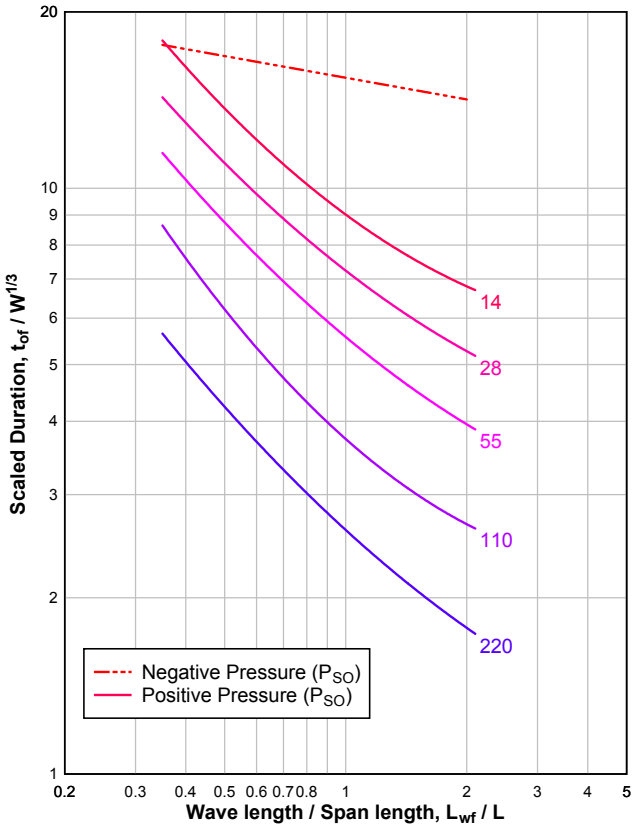

Figure 23: Scaled duration of positive and negative phase pressure loading for the roof and side-walls of a structure (modified from [9]).

3.2.4 Pressure on the rear wall

The rear wall of the structure is the last surface that is loaded from the propagation of the blast wave because of the secondary waves that are created when the blast front overpasses the roof and side walls. The secondary waves that are initiated from the roof are reinforced by their reflection on the ground, whereas the waves that are created from the side walls are reinforced due to their mutual impact at the middle of the distance between the two side wall edges.

The simplified calculation of the loading that is generated by these waves is similar to the one already presented for the roof and the side walls in Figure 20. An equation similar to Equation (16) can be used that involves the peak pressure values at the back edge of the roof slab. The final load at the rear wall is a combination of the incident and the drag pressure values. The drag pressure coefficients C_D, which are used for the dynamic component of Equation (16) are identical to the ones presented for the roof and the side walls at Table 3, while the dynamic pressure q_o corresponds to the pressure $C_E P_{sob}$ (relevant to point *b* at the back edge of the roof, Figure 20).

3.3 Influence of openings

Modern buildings are characterized by large openings, especially at their front side, to ensure adequate lightening and ventilation of interior spaces. Windows are the first elements that will potentially fail after a blast wave impinges on the surface of a building as they usually form the most vulnerable part of a structural face. Even if designed to sustain certain pressure values, the current philosophy behind structural design dictates that they form the weakest part of the wall system, as failure of the wall before failure of the glass façade is considered more hazardous.

Building exterior walls are likely to contain openings either on all sides, if the structure is not in contact with other buildings at its perimeter, or mainly on the front side. Most of the times the behaviour under blast loading of buildings containing openings on all sides, resembles that of buildings with openings only on the front. The reason for this behaviour is attributed to the fact that the internal partitions of the structure act as side and rear walls restricting the flow of the blast wave through the building. The blast wave front upon contact with a normal window will instantly cause its failure and it will extend in the interior of the building. At the same time the peak value of the pressure wave will get smaller as some energy will be absorbed by the glass breakage. Nevertheless, the pressure may eventually increase as the blast wave comes to contact with the interior partitions which lead to its reflection and consequently to a pressure rise.

Generally, blast pressures acting on the external surface of the walls are directed towards the interior of the structure. On the other hand pressures acting on the internal surface of the roof, the front, side or rear walls, due to the blast wave propagation within a structure after the failure of windows, are directed towards the outer environment. This means that the external and internal loads produced at these structural elements have opposite directions. Thus depending upon the design objective, two alternatives can be followed: i) As has already been pointed out, if the overall movement of the structure is to be evaluated, the total load produced due to the pressures acting on the outer surfaces of the front, the roof, side and rear walls should not be decreased. As a consequence, the pressures produced within a structure could be neglected. ii) However, whenever the motion of specific components or the outward motion of the surrounding walls has to be determined, the pressures produced at the interior of a building because of the presence of openings must be taken into account. These internal pressures should be properly added to the ones produced from the negative phase of the pressure time history at the outer surfaces of the structural elements.

A procedure for calculating the loads at the interior surfaces of the roof, the front, side and rear wall is proposed in [8]. No details are provided here and only some of its steps are outlined below. Thus, in order to determine the combined loading effect of the pressures acting on the external and the internal face of a wall, the time delay because of the time required for the windows breakage and the wave propagation inside the building should be taken into account. The several openings existing at the front façade of a building should be combined composing a single opening to be placed at the center of the wall, with an area equal to the total area of all the openings, while a new clearing time should be calculated. The value of the maximum pressure acting on the interior surface of a wall depends on the

peak pressure and wavelength L_w of the incident wave that acts on the external surface and the geometry of the building. All these values are provided by relevant diagrams contained in [8-9] and should be considered if failure of the surrounding windows is expected.

No further analysis will be made concerning the openings at a building during a blast event at the current report, as usually during design it is predominantly the positive phase of a pressure time history that is crucial. The loads acting on the walls during this phase are, in the majority of the cases, larger than those initiated from the combined effect of the negative phase at the outer surface and the pressures acting on the interior faces due to window failures.

3.4 Combination rules

The load combinations that have to be applied for a building designed for an accidental action, such as blast loading, are included in Eurocode EN-1990 [14]. According to its provisions the self-weight of the structure should be included, as well as the frequent of quasi-permanent values of the live and the snow load, if applicable. The wind and seismic loads may be neglected as their simultaneous presence with the accidental load is highly unlikely. Internal explosions that could be produced from a gas leakage are considered as a random effect in time. On the other hand, a terrorist attack is not strictly random, since it is not based on climate or random conditions, but could be the outcome of human planning. For this reason the designer should consider the probability of having to increase the safety factors proposed by the Eurocode, so as to take into account the individual requirements of the project under design, such as the expected occupancy at the time of the attack, the type and use of the building etc. The general formula proposed by [14] for the actions that have to be considered for the accidental combination is presented in Equation (17).

$$E_d = G + A_d + (\psi_1 or\ \psi_2)Q_{k,1} + \sum \psi_2\, Q_{k,i} \tag{17}$$

where, G is the self-weight of the structure,

A_d is the design value of the accidental action (in this case the blast load),

$Q_{k,1}$ is the characteristic value of the leading variable action and

$Q_{k,i}$ are the characteristic value of the accompanying variable actions.

The values of ψ_1 and ψ_2 depend on the relevant accidental design situation. In case of potentially targeted building structures ψ_1 ranges from 0.5 (for office and residential areas) to 0.7 (for congregation and shopping areas), while ψ_2 ranges from 0.3 to 0.6, respectively.
The explosion loads A_d to be used in the above action combination formula are specified for building internal explosions in Eurocode EN1991-1-7 [1]. No explosion loads are however provided for the case of external explosions. The information collected and presented in the previous sections attempts exactly to fill in this gap.

4. Summary of the blast loads calculation

1. An explosion scenario is agreed upon, thus defining the expected charge weight, type and detonation distance according to the geometry around the building (minimum possible approaching distance, interfering obstacles between the detonation point and the structure etc.). Charge weight should be compatible with the size of the vehicle that could possibly be used as means of transport. A judgment should be also made whether the blast is to be considered as a ground or as an air burst.
2. If multiple detonation locations exist, separate analyses should be performed for every case, as different parts of the structure may be loaded in each case.
3. The loaded surfaces of the structure are divided in as many sections as the engineer deems suitable. The blast parameters have to be computed for every such surface-section, as these are characterized by different distances from the blast source and possibly different areas. An easier approach is to use common parameter values for grouped together surface-sections, as long as the most conservative values are utilized. This procedure leads to overdesigning certain parts of the structure.
4. The equivalent TNT weight W is computed through Equation (5) and Tables 1 or 2. Alternatively, several graphs contained in [8-9], which describe some basic blast parameters (peak positive incident pressure, scaled impulse) of other explosive materials, may be used.
5. The scaled distances are next determined for every case scenario according to Equation (4). Depending on the expected type of blast wave (hemispherical from ground burst or spherical from air burst) the parameters are evaluated from the graphs of Figures 13 and 14. These include the peak incident P_{so} and reflected P_r pressures, the incident i_s and reflected i_r impulse, the wave front speed U, the duration of the positive phase t_o, the arrival time t_A and the wave length L_w. All these values (except for the pressures and velocities) are scaled to the $W^{1/3}$. In order to produce their absolute values they should be multiplied by $W^{1/3}$.
6. The next step includes the construction of the idealized triangular pressure diagrams for the structural surface-sections. For the front wall and the positive pressure wave duration, the clearing time t_c is computed via Equation (13), where the sound velocity C_r is determined from Figure 17. The fictitious duration t_{of} of the positive phase should next be estimated by using Equation (14) and also the fictitious duration t_{rf} of the reflected pressure via Equation (15). Since the peak incident pressure P_{so} at the section of interest has already been found, the peak dynamic pressure q_o can also be calculated from Figure 11. The value of $P_{so}+C_D q_o$ is thus determined by using $C_D=1$ for the drag coefficient for the front face of the structure. A diagram similar to that of Figure 19 is produced from which the load acting on the front surface can be defined by choosing the appropriate curve, i.e. that of the smallest impulse, as discussed in Section 3.2.
7. In case that the overall behaviour of the front wall under the blast wave is of interest, the negative phase of the blast wave should also be taken into account. The blast parameter values, such as the peak negative incident and normal reflected pressure and the scaled negative incident and normal reflected impulses should be computed by using the diagrams in Figure 15a and 15b. In order to obtain absolute values, the scaled impulses must be multiplied by $W^{1/3}$. The fictitious duration t_{rf}^{-} of the negative

phase reflected pressure is calculated by using Equation (15) and the corresponding negative phase quantities. The time where the minimum pressure value should be assigned is equal to t_o+0.25t_{rf}^-. This procedure produces the idealized triangular negative phase diagram of Figure 19, from which the suction force applied to the front surface can be computed.

8. The load applied to the roof or to the side walls of the structure is determined through a similar procedure. The equivalent positive C_E and negative phase C_E^- load factors, the rise time t_d and duration t_{of} are determined from Figures 21, 22 and 23. To obtain absolute values, scaled parameters should be multiplied by $W^{1/3}$. For calculating the required wavelength-span ratio L_{wf}/L, the wavelength and the incident pressure at the edge of the roof (or side wall) situated closer to the explosion are determined from Figure 13 or 14. The dynamic pressure q_o can be calculated from Figure 11 using the appropriate incident pressure. The value of the coefficient C_D is chosen from Table 4. A similar procedure is followed for the definition of the negative phase pressure-time curve. The corresponding rise time is equal to 0.25t_{of}^-, where t_{of}^- is the negative phase fictitious duration. Finally, a diagram similar to the one presented in Figure 20 is produced, from which the total load acting on the side walls or roof can be computed.
9. The loads acting at the rear wall of the structure can be similarly determined. The main difference is that the peak incident pressure P_{sob}, corresponding to the rear edge of the roof, is used as the basis.
10. The loads computed for every surface of the structure should be appropriately inserted in load combination rules, like the ones proposed in EN1990 and EN1991, in order to be applied during the structural design of the building. Depending on the building's category different types of analysis may be required, with structures of high importance possibly requiring comprehensive calculations using dynamic and non-linear analysis.

Figure 24 shows schematically the recommended procedure for constructing the pressure time history of a blast wave acting on the front face of a building.

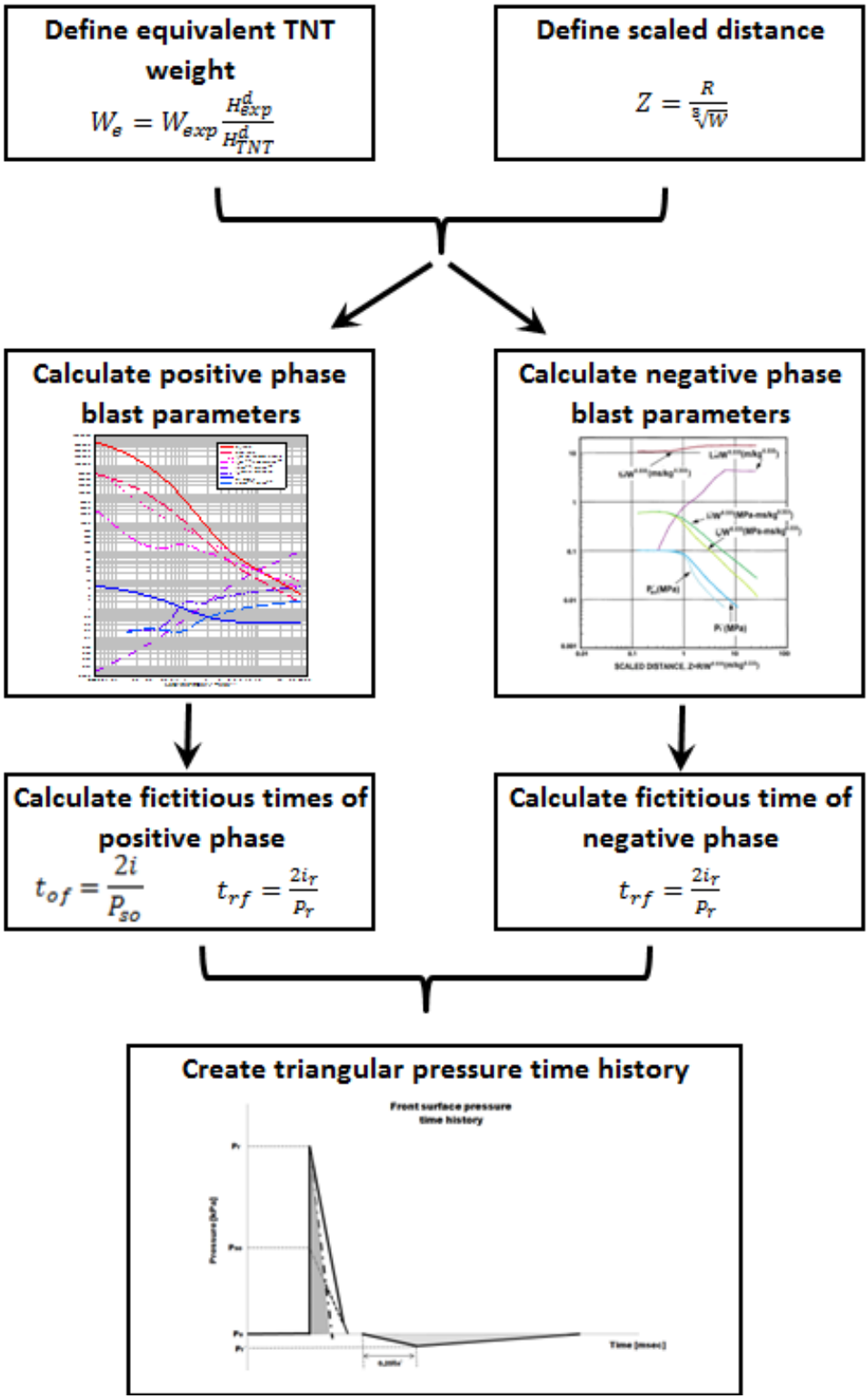

Figure 24: Diagram of pressure variation calculation for the front face of a structure.

5. Case studies

In this chapter the procedure of pressure and impulse calculation and their spatial distribution will be illustrated by examining typical explosion scenarios and structures of relatively simple geometry, which are subjected to the induced blast loading. No safety factor (increase of 20%) is applied to the charge weights.

5.1 Blast parameter calculation examples

In the following case study the blast parameters for points located either in mid-air or on the ground will be computed for an air blast and a surface burst.

i) Initially a blast is supposed to have taken place in mid-air, as can be seen at Figure 25. The blast wave is formed by an explosion of 750kg of TNT, which is situated 20m above the ground. The blast parameters will be determined for three locations. The first (point A) is 10m lower than the detonation point at an angle of 40°, the second (point B) is on the ground at an angle of 30° and the third (point C) is on the ground at an angle of 60°.

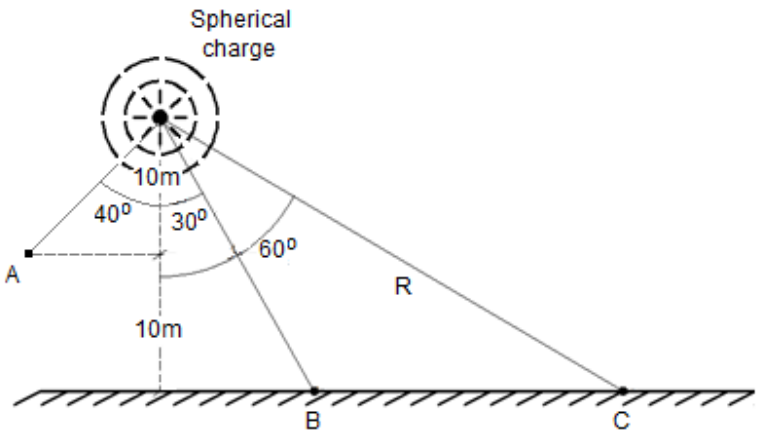

Figure 25: Distance of points A, B and C from a mid-air blast source.

Point A. Distance from detonation center: 10/cos40^o=13.05m

Scaled distance: $Z = \frac{R}{\sqrt[3]{W}} = \frac{13.05}{\sqrt[3]{750}} = \frac{13.05}{9.086} = 1.44$ m/kg$^{1/3}$

From Figure 13 the relative values are read and the calculated positive phase blast parameters for point A are reported below.

P_{so}= 409.5 kPa

i_s = 125.2 *750$^{1/3}$ = 1137.5 kPa-ms

t_o= 1.68 *750$^{1/3}$ = 15.3 ms

t_A= 1.06 * 750$^{1/3}$ = 9.6 ms

U= 0.72 m/ms

L_w= 0.38*750$^{1/3}$= 3.5 m

Point B. Distance from detonation center: 20/cos30^o=23.09m

Scaled distance: $Z = \frac{R}{\sqrt[3]{W}} = \frac{23.09}{\sqrt[3]{750}} = 2.54$ m/kg$^{1/3}$

Since α=30°, regular reflection takes place at B. Using Figure 13, it can be found that:

P_{so}= 115.5 kPa

i_s = 74.47 *750$^{1/3}$ = 676.6 kPa-ms
t_o= 2.39 *750$^{1/3}$ = 21.7 ms
t_A= 3.0 * 750$^{1/3}$ = 27.2 ms
U= 0.48 m/ms
L_w= 0.7*750$^{1/3}$= 6.3 m

From Figure 6 the reflection coefficient $C_{r\alpha}$ is calculated:

$C_{r\alpha}$ = 2.75 → $P_{r\alpha}$ = 2.75*115.5= 317.6 kPa,

and from Figure 8b the reflected impulse is:

$i_{r\alpha}$ =180 *750$^{1/3}$ =1635.4 kPa-ms.

Point C. Distance from detonation center: 20/cos60^o=40.00m

Scaled distance: $Z = \frac{R}{\sqrt[3]{W}} = \frac{40.00}{\sqrt[3]{750}}$=4.40 m/kg$^{1/3}$

Using Figure 13 as before, the parameters of the incident wave at C can be readily found:

P_{so}= 39.1 kPa
i_s = 45.70 *750$^{1/3}$ = 415.2 kPa-ms
t_o= 3.18 *750$^{1/3}$ = 28.9 ms
t_A= 7.4 * 750$^{1/3}$ = 67.2 ms
U= 0.39 m/ms
L_w= 1.0*750$^{1/3}$= 9.0 m

Since α=60° > 40° ≈α_{crit}, a Mach stem will be formed upon the reflection of the wave from the ground at C, the characteristic parameters of which will be determined below.

For α=60° and P_{so}= 39.1 kPa the coefficient $C_{r\alpha}$ is calculated, Figure 6:

$C_{r\alpha}$ = 2.55 → $P_{r\alpha}$ = 2.55*39.1= 99.7 kPa,

and from Figure 7b the reflected impulse is:

$i_{r\alpha}$ =70 *750$^{1/3}$ =636.0 kPa-ms.

The calculated peak reflected pressure $P_{r\alpha}$ will constitute the peak incident overpressure P_{soM} of the Mach stem pressure-time curve, i.e.

P_{soM} = 99.7 kPa,

and the reflected impulse $i_{r\alpha}$ will be the corresponding incident positive pulse i_{sM}^+, i.e.

$i_{sM}^+ = i_{r\alpha}$ =636.0 kPa-ms.

The other characteristics of this Mach front are determined as follows:

For the incident impulse of 636.0 kPa-ms (not scaled value), from Figure 13 a fictitious scaled distance Z_{f1} and the positive phase duration t_{oM} are found:

Z_{f1}= 2.72 m/kg$^{1/3}$
t_{oM} = 2.5 * 750$^{1/3}$= 22.7 ms.

The determination of the other parameters is based on the incident overpressure. Specifically, for P_{soM}=99.7 kPa, from Figure 13 a fictitious scaled distance is found

Z_{f2}=2.72 m/kg$^{1/3}$,

from which the values of the arrival time, shock wave speed and wavelength are, respectively, determined:

t_A= 3.4 * 750$^{1/3}$ = 30.8 ms,
U= 0.46 m/ms,
L_w= 0.7* 750$^{1/3}$= 6.4 m

Referring to Figure 7, this approach is used in order to define the parameters of the incident pressure pulse for structures that lie within the Mach front in case of explosions that take place at a certain distance from the ground. If part of the structure lies over the triple point of the Mach front, it will undergo a different pressure variation, characterized by two peaks (of lower amplitude) and increased time duration. Usually, it is on the conservative side to consider a uniform incident pressure over the whole front surface, which is equal to that of the Mach front just ahead of the building. Figure 7 (bottom) can provide an estimate of the height of the triple point. Entering the values of $R_G/W^{1/3}$ =34.64/9.086 =3.8 and $H_c/W^{1/3}$ =20/9.086 = 2.2, it can be easily found that the height of the Mach front in this case is approximately H_T= 0.15* $750^{1/3}$=1.36 m, which is indeed quite low.

Note. An alternative approach for the determination of the reflected blast parameters at point C is through the use of diagrams 2-9 and 2-10 of references [8,9]. These diagrams show the peak reflected pressure or reflected impulse as functions of the scaled height of charge from the ground and of the angle of incidence. Thus, P_{soM} and i_{sM}^{+} would be found, while the rest would follow the same steps.

ii) If we are dealing with a surface blast the procedure of determining the blast parameters is more straightforward. In Figure 26 a hemispherical blast wave is produced from a 100kg TNT detonation and the blast parameters at point C will be determined.

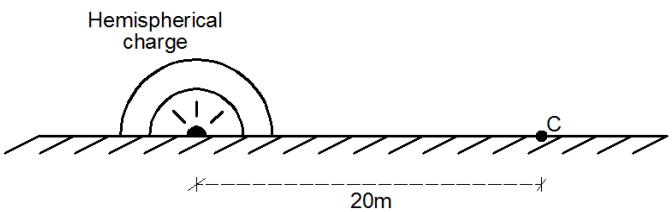

Figure 26: Distance of point C from a surface blast source.

Scaled distance: $Z = \frac{R}{\sqrt[3]{W}} = \frac{20.0}{\sqrt[3]{100}}$=4.31 m/kg$^{1/3}$

From Figure 14 the peak incident pressure P_{so}, the incident impulse i_s, the arrival time t_A and the positive phase duration t_o can be calculated, and are shown in the following table. Where needed, parameters are multiplied by $W^{1/3}$ in order to get their absolute values. The negative phase parameters can be computed using the same principle according to the relative diagrams contained in [8].

Point C	Incident pressure P_{so} [kPa]	Positive incident impulse i_s	Arrival time t_A	Positive duration t_o	Shock wave speed U[m/ms]	Wavelength L_w
Diagram read scaled values	56.00	67.00	6.60	3.55	0.41	1.00
Absolute values	56.00	310.51	30.59	16.45	0.41	4.63

5.2 Blast wave pressure loads for a small structure

Figure 27 shows the small building configuration that will be considered, which is an isolated structure, situated at a certain distance from the assumed detonation point. As can be seen, the structure has a standoff distance of 27m from a truck, which is assumed to carry a charge of 1000kg of C4. This is one of the most common types of plastic explosive material, it is very stable and it cannot be detonated without the use of a detonator. The building is situated directly across the blast point and its dimensions are 6mx3.1mx6m. The blast load will be evaluated at (the center of) the front surface, which has an area of 18.6m^2 (6x3.1m) and lies normal to the blast wave propagation direction. Except from the reflected pressures at the front face of the building, the pressures at the roof, the side and rear walls will be also computed.
The explosive is detonated almost at ground level so a hemispherical blast wave will be produced. The distance from the blast point is considered large enough, so as to assume that the blast wave impinging on the structure is plane and the pressure applied is uniform across the front surface.

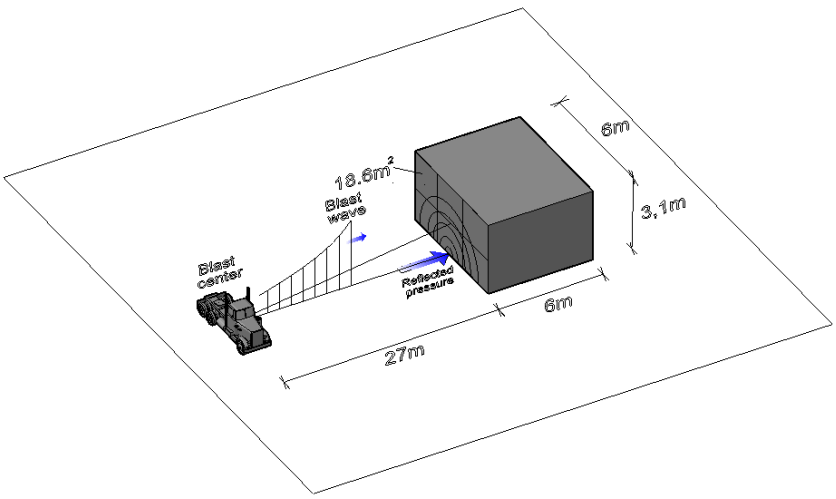

Figure 27: Geometry of blast site.

The charge weight of W_{exp}=1000kg of C4 must be converted to an equivalent charge of TNT according to Equation (5) and Table 1:

$$W = W_{exp}\frac{H^d_{exp}}{H^d_{TNT}} = 1000kg\frac{H^d_{C4}}{H^d_{TNT}} = 1000\frac{5.86}{4.50} = 1302 \text{ kg}$$

The value of the TNT equivalent mass will differ slightly if the predefined TNT equivalence factors proposed in other sources are used. Quite often two values for the equivalent factor of an explosive are quoted (Table 2), one referring to equivalence with respect to peak overpressure and the other to equivalence with respect to positive impulse. In this case their average may be used for defining the equivalent TNT mass of the explosive.

<u>Front wall pressure</u> Front surface center height: *h*=1.55m

Distance from blast source: $R_h = \sqrt{(27^2 + 1.55^2)} = 27.04 \text{ m}$

Scaled distance: $Z = \frac{R_h}{\sqrt[3]{W}} = \frac{27.04}{\sqrt[3]{1302}} = 2.56$ m/kg$^{1/3}$

Angle of incidence: equation $a_1 = \arctan\left(\frac{h}{R}\right) = 4^o < 40^o$

The angle of incidence is small and a lot smaller than 40 degrees. So, according to Figure 6, regular reflection environment is expected with conditions not differing from those of the normal reflection. So the use of the normal reflected pressure for the building is justified as it will lead to slightly conservative results.

The diagrams of Figure 14 (which are for zero angle of incidence) can be directly used for the calculation of the blast parameters and the results are shown at the table below. Clearly, for obtaining absolute values, multiplication by $W^{1/3}$ has been effected, where needed.

Front face	Incident pressure Pso [kPa]	Positive incident impulse İs	Reflected pressure Pr [kPa]	Positive reflected impulse ir	Arrival time	Positive duration	Shock wave speed U [m/ms]	Wavelength Lw
Diagram read scaled values	160.00	105.00	500.00	270.00	2.80	2.40	0.51	0.66
Absolute values	160.00	1143.81	500.00	2878.63	29.85	25.59	0.51	7.19

Velocity of sound, Figure 17: C_r =0.45 m/ms

Clearing time: $t_C = \frac{4S}{(1+R)C_r} = \frac{4*3}{(1+0.968)0.45} = 13.5$ ms

Fictitious positive phase duration: $t_{of} = \frac{2i_s}{P_{so}} = \frac{2*1143.81}{160.0} = 14.30$ ms

Fictitious duration of reflected pressure: $t_{rf} = \frac{2i_r}{P_{ra}} = \frac{2*2878.63}{500} = 11.51$ ms

Peak dynamic pressure, Figure 11: q_o= 65 kPa

Drag coefficient for building front wall: C_D= 1.0

Reduced peak pressure, Equation (12): $P_{so}+C_Dq_o$= 160+(1.0*65.0)=225 kPa

After defining these parameters, according to Section 3.2.2 the positive phase of the two alternative pressure curves for the front of the building can be graphically represented in Figure 28. As can be seen from this figure, the fully reflected pressure time curve will be used for the building design loads as its impulse (shaded area) is smaller than the impulse of the curve computed through the use of the clearing time.

If the overall behaviour of the structure to blast loading is needed and not only the maximum frontal impulse and pressure, the negative phase parameters of the blast load should also be determined. The diagrams of Figure 15b are used, and the values of the parameters are shown in the next table. By using these parameters, the entire pressure time curve over the whole duration (positive+ negative phase) of the blast wave can be constructed, as seen in Figure 28. It is recalled that the negative phase curve begins exactly after the end of the positive phase duration t_o and that its rise-time is equal to $0.25t_{of}^-$= 0.25*174.71=43.68ms.

Front face	Incident negative pressure Pso⁻ [kPa]	Negative incident impulse is⁻	Reflected negative pressure Pr⁻ [kPa]	Negative reflected impulse ir⁻	Negative duration to⁻	Negative wavelength Lw
Diagram read scaled values	16.50	0.13	30.00	0.20	16.00	1.90
Absolute values	16.50	1419.50	30.00	2183.90	174.71	20.70

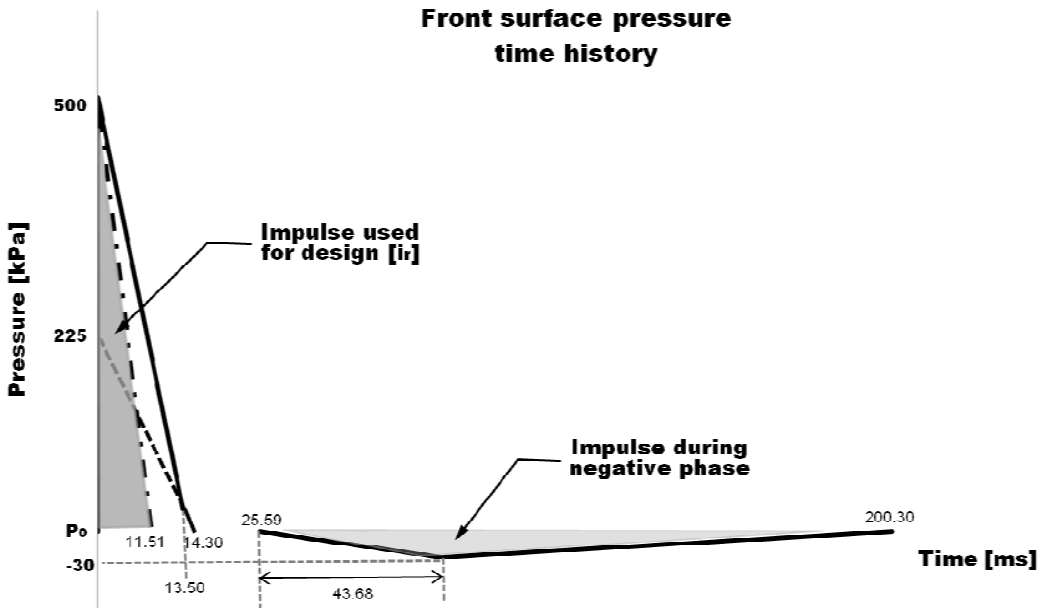

Figure 28: Blast pressure time history at front wall of the structure.

The same procedure is followed for the computation of the loads acting on the side and rear walls as well as on the roof of the structure. Even though the most important loading in terms of maximum loading values, is the one acting at the front face of the building, the determination of the loads acting on all of the external faces is important if the overall behaviour of the building to the blast is of interest or if the design of individual members is of concern. Usually, if the front face of a structure is able to withstand the blast wave, the rest of the structure will also be able to remain structurally unharmed as the loads acting on the rest of the surfaces are smaller, compared to those at the front.

<u>Roof pressure</u> For the roof of the building the calculations start with reference to its edge nearer to the blast source (point *f* in Figure 20). The peak incident pressure at this location is equal to that of the front face, i.e.,

P_{sof} =160 kPa.

Based on that, the wavelength at point f is determined from Figure 14, and the ratio L_{wf}/L is calculated,

L_{wf} = 7.62 m → L_{wf}/L= 7.62/6.00 = 1.27.

For the positive phase pressure the equivalent positive phase load factor C_E is found from Figure 21,

C_E =0.53,

and the dynamic pressure q_o, corresponding to incident pressure $C_E P_{sof}$ =84.8kPa, is determined from Figure 11,

q_o = 20 kPa.

Using from Table 4 drag coefficient C_D= -0.4, Equation (16) yields the maximum positive roof pressure

P_R = 84.8 - 0.4*20 = 76.8 kPa.

The rise time t_d, and the overall duration of the positive phase t_{of} are also determined from the relevant diagrams of Figures 22 and 23,

t_d = 13.10 ms ,

t_{of} = 31.67 ms.

Parameters read from diagrams have been multiplied by $W^{1/3}$ in order to derive their absolute values, where needed.

Roof	Wavelength Lw	Ratio Lw/L	Equivalent positive phase load factor C_E [-]	Duration of rise time td	Duration of equivalent uniform pressure tof	$P_r=C_E P_{sof}$ [kPa]	Peak positive pressure [kPa]
Diagram read scaled values	0.70	-	0.53	1.20	2.90	-	-
Absolute values	7.64	1.27	-	13.10	31.67	84.80	76.80

In order to compute the negative phase parameters a similar procedure is followed by reading the same diagrams, which also contain data for the negative phase of the blast wave. The negative phase starts at time t_o= 25.59 ms, calculated above.

Thus the equivalent negative phase load factor C_E^- is found from Figure 21,

C_E^- = - 0.26,

and the peak negative roof pressure is calculated as

$P_R^- = C_E^- P_{sof}$ = - 0.26*160 = - 41.6 kPa

The overall duration of the negative phase t_{of}^- is derived from Figure 23

t_{of}^- = 180.17ms

and the corresponding rise time t_d^- is computed with the formula

$t_d^- = 0.25\, t_{of}^-$ = 0.25* 180.13 = 45.04 ms

It is noted that the negative phase peak pressure depends only on the incident pressure P_{sof} and not on its combination with the dynamic pressure q_o.

Roof	Wavelength Lw	Ratio Lw/L	Equivalent negative phase load factor C_E^-	Duration of equivalent uniform negative pressure t_{of}^-	Duration of negative phase rise time t_d^-	Negative phase reflected pressure $P_r=C_E^- P_{sof}$ [kPa]
Diagram read scaled values	0.70	-	0.26	16.50	-	-
Absolute values	7.64	1.27	-	180.17	45.04	41.60

Based on the parameters determined, the triangular diagrams of the positive and negative phases of the pressure-time variation are presented in Figure 29. This is the pressure to be applied uniformly over the whole roof surface. For clarity in Figure 29 the origin of time has been set to the arrival time (t_A) of the wave at the front face of the building.

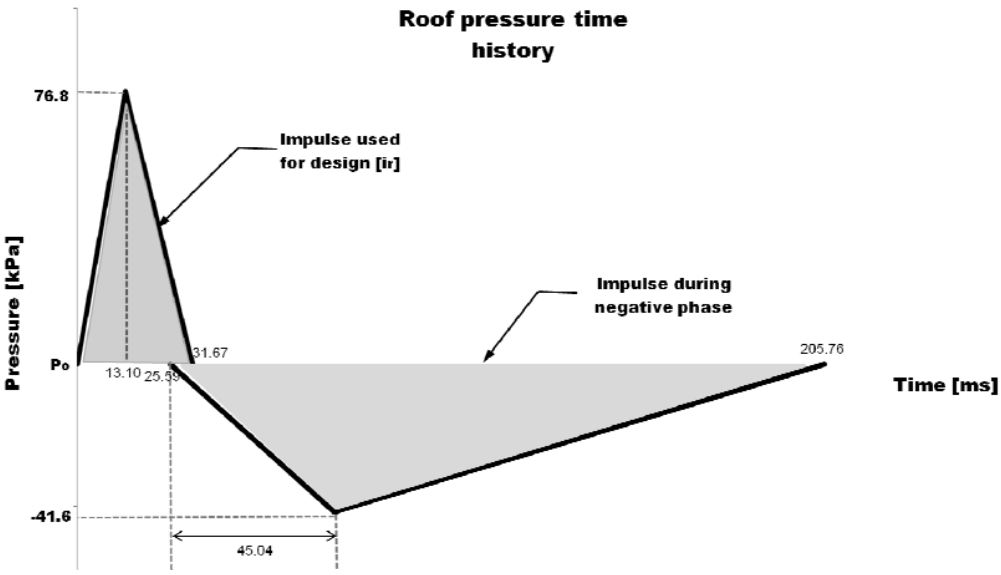

Figure 29: Blast pressure time history at the roof of the structure.

Side wall pressure The pressure time history for the side walls of the structure is identical to the one already derived and shown in Figure 29, because the blast parameters are the same, as long as the front edge of the roof is used as reference for the derivation of these values. On the contrary, for the rear wall of the structure the parameters will be different because the distance from the blast source increases.

Rear wall pressure For the rear wall of the building the calculations start by taking as reference the back edge of the roof (point *b* in Figure 20). The distance from the explosion source is 27+6=33m, thus the scaled distance, arrival time and peak incident pressure there are (Figure 14), respectively,

Z= 33/(1302)$^{1/3}$ = 3.02 m/kg$^{1/3}$,

t_A= 3.5*(1302)$^{1/3}$ =38.2 ms ,

t_o= 2.95*(1302)$^{1/3}$ =32.21 ms,

P_{sob} = 120 kPa.

From Figures 22 and 23, the rise time and overall duration of the positive phase are:

t_d = 0.75 * (1302)$^{1/3}$ = 8.19 ms

t_{of} = 2.30 * (1302)$^{1/3}$ = 25.11 ms

The wavelength at point *b* is also determined from Figure 14, and the ratio L_{wf}/L is calculated

L_{wb} = 0.76 * (1302)$^{1/3}$ = 8.30 m → L_{wb}/L = 8.30/3.10 = 2.68

From Figure 21:

C_E =0.76,

therefore $C_E\ P_{sob}$ =91.2 kPa and from Figure 11:

q_o = 28.0 kPa

From Table 4: C_D= - 0.4, and the maximum positive rear wall pressure is:

P_{rw} = 91.2 - 0.4*28 = 80.0 kPa

The following table contains the values of the calculated blast parameters for the positive pressure phase.

Rear wall	Incident pressure [kPa]	Wavelength Lw	Ratio Lw/L	Equivalent positive phase load factor C_E [-]	Duration of rise time td	Duration of equivalent uniform pressure tof	$P_r=C_EP_{sof}$ [kPa]	Peak positive pressure [kPa]
Diagram read scaled values	120.00	0.76	-	0.76	0.75	2.30	-	-
Absolute values	120.00	8.30	2.68	-	8.19	25.11	91.20	80.00

A similar approach is used for the derivation of the negative blast phase parameters, which are included in the following table. Based on these data, the graph of Figure 30 is constructed, which shows the entire pressure time history at the rear wall. The origin of time in Figure 30 has been set at the arrival time (t_A) of the wave at the rear wall (point *b*). In order to compare this curve with those of the front wall, side walls and roof, and for consistency in the timing of load application, this origin has been displaced to the right by 8.37 ms (=38.22-29.85). This is the delay in the arrival times of the wave to the front (f) and the back (b) face of the building.

Rear wall	Wavelength Lw	Ratio Lw/L	Equivalent negative phase load factor C_E^- [-]	Duration of equivalent uniform negative pressure t_{of}^-	Duration of negative rise time t_d^-	Negative phase reflected pressure $P_r=C_E^-P_{sof}$ [kPa]
Diagram read scaled values	0.76	-	0.28	15.00	-	-
Absolute values	8.30	2.68	-	163.79	40.95	33.60

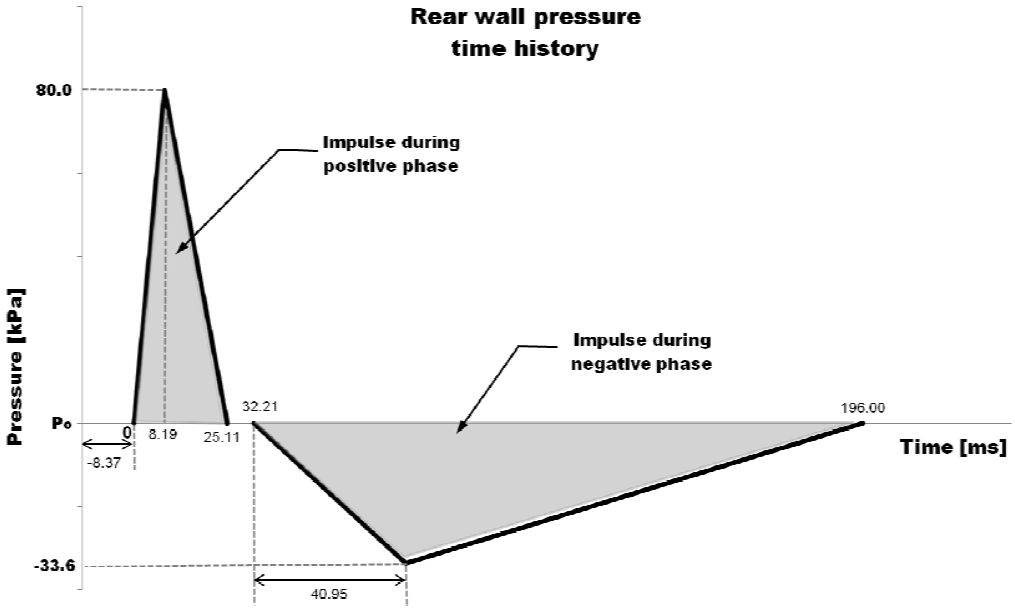

Figure 30: Blast pressure time history at the rear wall of the structure.

5.3 Blast wave pressure loads for element design

The current case study focuses on the calculation procedure of blast pressure time histories for structural or non-structural elements along the height of a building. The geometry of the explosion site is represented in Figure 31 and is composed of a vehicle carrying 1000kg of TNT at a distance of *R*=15m from a 20m-high building. The front face of the building is made of 15 panels. The blast load will be evaluated at five different locations along the middle panel strip, so as to compare the effect of the distance and incidence angle of the panel surface from the explosion's center. Each one of the five surfaces (panels) has an area of 16m^2 (4mx4m). The first lies normal to the blast wave propagation direction at the bottom of the front surface, whereas the others stretch to the top of the building's front façade spaced 4m from each other, as can be seen in Figure 31. In this study only the positive phase parameters of the blast wave at the front face of the structure will be considered.

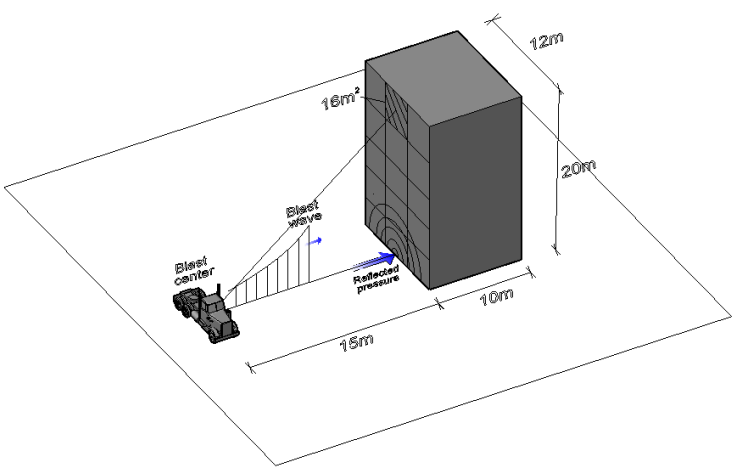

Figure 31: Geometrical configuration of blast site.

The blast parameters will be calculated with reference to the height *h* of the center of each of the five areas, which ranges from 2m (Area-1) to 18m (Area-5). If the detonation is assumed to be taking place at ground level, the actual distances and the scaled distances for each panel-centroid are computed according to equations $R_h = \sqrt{(R^2 + h^2)}$ and $Z = \frac{R}{\sqrt[3]{W}}$, respectively. The angle of incidence for each of these locations is computed through equation $\alpha = \arctan\left(\frac{h}{R}\right)$.

	Surface's height [m]	Distance from blast source [m]	Scaled distance [m/kg$^{1/3}$]	Angle of incidence [deg]
Area-1	2.0	15.1	1.52	7.6
Area-2	6.0	16.2	1.62	21.8
Area-3	10.0	18.0	1.81	33.7
Area-4	14.0	20.5	2.06	43.0
Area-5	18.0	23.4	2.35	50.2

A simplified procedure is applied first, which uses the fully normal reflected pressure at zero angle of incidence corresponding to the scaled distance from the blast source. The blast parameters are derived using the diagrams of Figure 14 for all areas in the front face of the building. The impulse, arrival time and duration of positive phase are scaled values, so in the following table they have been multiplied by $W^{1/3}$ in order to derive their absolute value.

Area-4 and Area-5, which are located at the top of the building's facade, have an angle of incidence which is larger than 40°, so the graph of Figure 6 could be used to establish whether the normal reflected pressure values calculated above are on the safe side. Clearly, by examining Figure 6, it can be deduced that the reflected pressure values for α=43° and α=50.2° are smaller than those calculated when using normal reflection (zero angle of incidence).

This more exact methodology is applied for all points, and through the diagram of Figure 6 the reflected pressures $P_{r\alpha}$ are calculated. Using these values and the curves of Figure 14 the corresponding positive reflected impulses are calculated and reported in the last column of the table below. Clearly in all cases the "exact" values are smaller than the corresponding ones produced by the normal reflection approximation.

	Incident pressure [kPa]	Positive incident impulse [kPa·ms]	Reflected pressure [kPa]	Positive reflected impulse [kPa·ms]	Arrival time [ms]	Positive duration [ms]	Reflected pressure coefficient Crα	Exact reflected pressure [kPa]	Exact positive reflected impulse [kPa·ms]
Area-1	530.00	1726.02	2400.00	4983.91	9.87	21.01	4.40	2332.00	4886.19
Area-2	460.00	1626.25	2000.00	4593.01	11.24	20.52	3.95	1817.00	4104.40
Area-3	355.00	1456.64	1420.00	4006.67	13.68	19.94	3.50	1242.50	3615.78
Area-4	265.00	1297.01	960.00	3420.33	17.59	20.13	3.22	853.30	3322.61
Area-5	200.00	1147.36	650.00	2931.71	22.28	21.30	2.20	440.00	2540.82

Figure 32 shows the distribution of the main blast parameters at the front face of the building at each of the five selected areas. If it is further desired to derive the corresponding pressure time history diagrams, the procedure that has already been introduced at the previous case study should be followed.

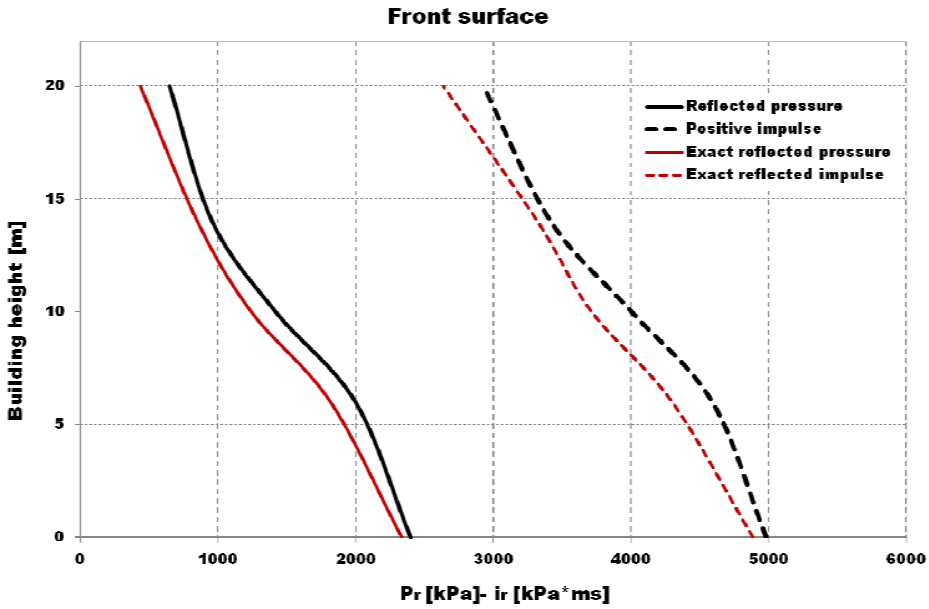

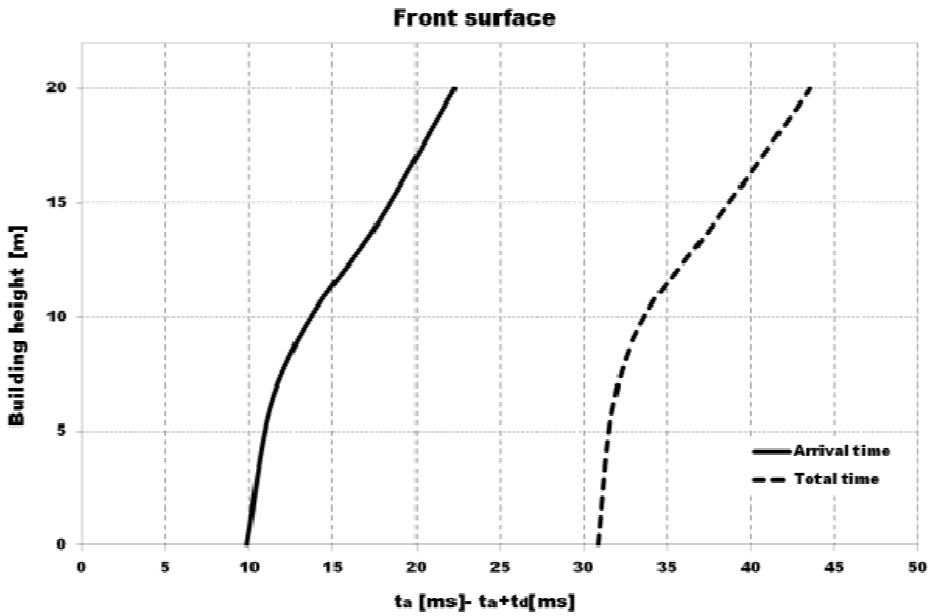

Figure 32: Distribution of blast parameters along the building's mid vertical strip of the front face.

6. Conclusions

Technical information has been collected, adapted and presented in this report for the calculation of the external explosion loads to be considered in the blast protection design of a structure. Empirical methods for the prediction of blast loads have been chosen as this is closer to the traditional engineering design approach. Thus several formulas, graphs and diagrams have been included, which make this guide sufficiently self-contained. Case studies have also been worked out in order to demonstrate through simplified examples the steps that must be followed for the calculation of blast pressures.

Of course more complicated cases of blast loading, where obstacles are involved and wave shadowing and channeling phenomena take place, cannot be handled through this approach. More comprehensive mathematical tools, e.g. explicit finite elements codes, will have to be employed for calculating blast pressures, at the expense of added complexity and computation time.

The material presented can help for introducing the subject, and in most cases it can form a basis allowing a reliable blast assessment of a structure to be initiated. This is important for design engineers, as the Eurocodes (EN 1991-1-7) do not yet deal with this type of loads and no relevant European guidelines are available.

7. References

[1] European Committee for Standardization (CEN) Eurocode 1: Actions on structures, Part 1-7: prEN 1991-1-7: "General actions-Accidental actions", 2006.

[2] Baker W.E., (1973) "Explosions in Air", Univ. of Texas Press, Austin TX USA.

[3] Kinney G. F., Graham K.J., (1985) "Explosive Shocks in Air", Springer, Berlin.

[4] Bulson P. S., (1997) "Explosive Loading of Engineering Structures", Chapman and Hall.

[5] Mays G.C., Smith P.D., (2001) "Blast effects on buildings - Design of buildings to optimize resistance to blast loading", Tomas Telford.

[6] Krauthammer T., (2008) "Modern Protective Structures", CRC Press, Taylor & Francis Group.

[7] Kingery C. N., Bulmash G., (1984) "Technical report ARBRL-TR-02555: Air blast parameters from TNT spherical air burst and hemispherical burst", AD-B082 713, U.S. Army Ballistic Research Laboratory, Aberdeen Proving Ground, MD.

[8] U.S. Department of the Army, (1990) "Structures to resist the effects of accidental explosions", Technical Manual 5-1300.

[9] Unified Facilities Criteria (2008), “UFC 3-340-02 Structures to Resist the Effects of Accidental Explosions“, U.S. Army Corps of Engineers, Naval Facilities Engineering Command, Air Force Civil Engineer Support Agency.

[10] International Ammunition Technical Guideline (IATG), Formulae for ammunition management 01.80, United Nations, 2011.

[11] Brode H. L., (1955) “Numerical solution of spherical blast waves”, Journal of Applied Physics, American Institute of Physics, New York.

[12] Newmark N.M., Hansen R.J., (1961) “Design of blast resistant structures”, Shock and Vibration Handbook, Vol.3, Eds. Harris & Crede, McGraw-Hill, New York.

[13] Mills C. A. (1987) “The design of concrete structures to resist explosions and weapon effects”. Proceedings of the 1st Int. Conference on concrete for hazard protections, Edinburgh, UK.

[14] European Committee for Standardization (CEN) Eurocode 0: Basis of Structural Design, EN 1990, 2005.

European Commission
EUR 26456 EN – Joint Research Centre – Institute for the Protection and Security of the Citizen

Title: Calculation of Blast Loads for Application to Structural Components

Authors: Vasilis Karlos, George Solomos

Luxembourg: Publications Office of the European Union

2013 – 58 pp. – 21.0 x 29.7 cm

EUR – Scientific and Technical Research series - ISSN 1831-9424

ISBN 978-92-79-35158-7

doi:10.2788/61866

Abstract

This technical report describes a procedure that can be followed for the calculation of the loads to be applied to a structure as a consequence of a blast. The report considers explosions taking place outside a building, which are not addressed directly at the relevant European Standards (Eurocode EN1991-1-7) dealing with accidental loading scenarios. The aim is the production of a simple, self-contained guide enabling the structural engineer to conduct a preliminary design of buildings for possible terrorist attacks. Aspects of the theory of blast waves have been included at an introductory level. The approach of the empirical methods for the prediction of blast loads has been chosen, which is more straightforward and has resulted from extensive experimental testing. For the determination of the main blast parameters, several graphs and diagrams have been included, which have been collected and properly adapted from several authoritative sources. This should make the load calculation procedure easier to grasp and less demanding in terms of mathematical complexity and computational capacity. Selected case studies are also presented in order to demonstrate through simplified examples the steps that must be followed for the calculation of blast pressures on the surfaces of a structure.

LB-NA-26456-EN-N

As the Commission's in-house science service, the Joint Research Centre's mission is to provide EU policies with independent, evidence-based scientific and technical support throughout the whole policy cycle.

Working in close cooperation with policy Directorates-General, the JRC addresses key societal challenges while stimulating innovation through developing new standards, methods and tools, and sharing and transferring its know-how to the Member States and international community.

Key policy areas include: environment and climate change; energy and transport; agriculture and food security; health and consumer protection; information society and digital agenda; safety and security including nuclear; all supported through a cross-cutting and multi-disciplinary approach.

Publications Office

ISBN 978-92-79-35158-7
doi:10.2788/61866